1970

A study of the effects of pressure-induced viscosity changes on the fluid flow characteristics in a circular tube

Robert Charles Weber

Department:

A STUDY OF THE EFFECTS OF PRESSURE-INDUCED VISCOSITY CHANGES ON THE FLUID FLOW CHARACTERISTICS IN A CIRCULAR TUBE

BY

ROBERT CHARLES WEBER, 1944-

A

THESIS

submitted to the faculty of

UNIVERSITY OF MISSOURI - ROLLA

in partial fulfillment of the requirements for the

Degree of

MASTER OF SCIENCE IN ENGINEERING MECHANICS

Rolla, Missouri

1970

Approved by

Robert L. Davis (advisor) Peter D. Hansen

T. F. Zehnhoff

ABSTRACT

A method of determining the response of fluids under high pressure to quick-release into the atmosphere is presented in this report. The analytical efforts have been formulated into two parts, a closed-form solution and a numerical analysis. By assuming constant viscosity of the fluid a closed-form solution was obtained. The assumption of constant viscosity was found to be acceptable for the test fluids up to an initial pressure of approximately 10,000 psi. A numerical analysis became necessary for initial pressures over 10,000 psi, where the variable viscosity of the fluid had to be considered.

The experimental work was conducted by observing the flow of a fluid from a pressurized reservoir through a circular tube to the atmosphere. The primary experimental variables were: (1) length of the circular tube, (2) type of fluid used, and (3) initial reservoir pressure. The pressure decay was measured by the use of strain gages in the reservoir and recorded on an oscilloscope screen.

ACKNOWLEDGEMENTS

The author is greatly indebted to Dr. Robert L. Davis, of the Department of Engineering Mechanics at the University of Missouri at Rolla, for his advice and aid in the formulation of this thesis, and for his guidance and valuable criticism throughout this research program.

The writer wishes to express his appreciation to Dr. Peter G. Hansen, of the Department of Engineering Mechanics, for his valuable aid in the taking of photographs necessary for this thesis.

The writer also wishes to express his thanks to the National Science Foundation for the support given to the author which made the research and this paper possible, and to Sun Oil Company, which so generously supplied the oil samples which made possible the experimental phase of this report.

TABLE OF CONTENTS

LIST OF ILLUSTRATIONS

LIST OF ILLUSTRATIONS (CONT.)

Figures Page

LIST OF TABLES

NOMENCLATURE

ρ	mass density of fluid	$slugs/in^3$
$\bar{v}$	velocity vector	in/sec
P	fluid pressure	psia
$\bar{F}$	body forces per unit mass	lb/slug
μ	coefficient of viscosity of fluid	$lb\text{-}sec/in^2$
ξ	vorticity vector	sec^{-1}
∇	operator del	
ν	kinematic viscosity of fluid	in^2/sec
u,v,w	radial, circumferential, and longitudinal velocities, respectively, of fluid within bore of pressure pot	in/sec
F_1, F_2, F_3	radial, circumferential, and longitudinal body forces per unit mass, respectively, acting on fluid in bore of pressure pot	lb/slug
Q	volume rate of fluid flow	in^3/sec
V	volume of fluid in compression chamber	in^3
θ	time constant	msec
K_p	fluid compressibility factor	in^2/lb
θ_1	circumferential direction	
P_g	pressure in pressure pot at time equal to zero	lb/in^2

I. INTRODUCTION

The increasing use of hydraulic systems of more complex design, ranging from hydraulically controlled equipment to fuel injection of diesel engines, has necessitated increasing research into high-pressure related phenomena. The dynamic behavior of fluids under extreme pressure (10,000 psi and above) is relatively unknown. At these extreme pressures the viscosity increase because of the increase in pressure is appreciable and must be included in any worthwhile analysis. This paper presents the results of an investigation of the effects of pressure-induced viscosity changes on the fluid flow characteristics in a circular tube.

The experimental work was conducted by observing the flow of a fluid from a pressurized (up to 50,000 psi) reservoir through a circular tube to the atmosphere. The fluid was released to the atmosphere by means of a quick release valve. As the fluid progresses from the reservoir to the atmosphere, the pressure decreases and creates a condition of variable viscosity along the tube length.

The purposes of this study are: (1) to find an analytical solution which gives realistic pressure, time, and velocity information for the flow of a variable viscosity fluid through a circular tube, and (2) to verify the solution with experimental results.

Among the best-known researchers in the high-pressure field are Mr. W.A. Wright (high-pressure bulk modulii work

with petroleum oils), Mr. J.D. Novak and W.O. Winer (high pressure research in the field of lubricant rheology), and Dr. R.L. Davis and Mr. M.D. Hersey(high pressure research in the field of fluid flow).

II. EXPERIMENTATION

A. EXPERIMENTAL FACILITIES

The experimental facilities consisted of three distinct parts (Fig. B-1): (1) the pressure pot and pump, (2) instrumentation, and (3) the quick-release mechanism. Although each of these parts performs a distinct function, their inter-relationship is necessary for a workable facility. In order to increase the understanding of the individual parts, each will be examined separately and in detail.

1. PRESSURE POT AND PUMP

The pressure pot and pump were mounted on a cart as one unit (Fig. B-2) with a 50,000 psi pressure gage connected directly to the chamber of the pressure pot. The top of the cart could be easily sealed off by sliding panels, and the doors on the front of the cart could be closed during testing for safety purposes. A cross-sectional view of the pressure pot is shown in Fig. 1.

The pressure pot was a two-piece, thick-walled vessel. The top plate was secured by ten (10) one-inch diameter, hardened, stainless-steel bolts. The high-pressure seal was obtained through the use of a metal "C" ring. Once the "C" ring has been seated and the bolts diametrically tightened, the top plate should not be removed since the seal can be disfigured or scarred, and proper sealing may not occur. If a long duration of time (e.g. overnight) existed between runs, a pressure of approximately 20,000 psi was maintained in the

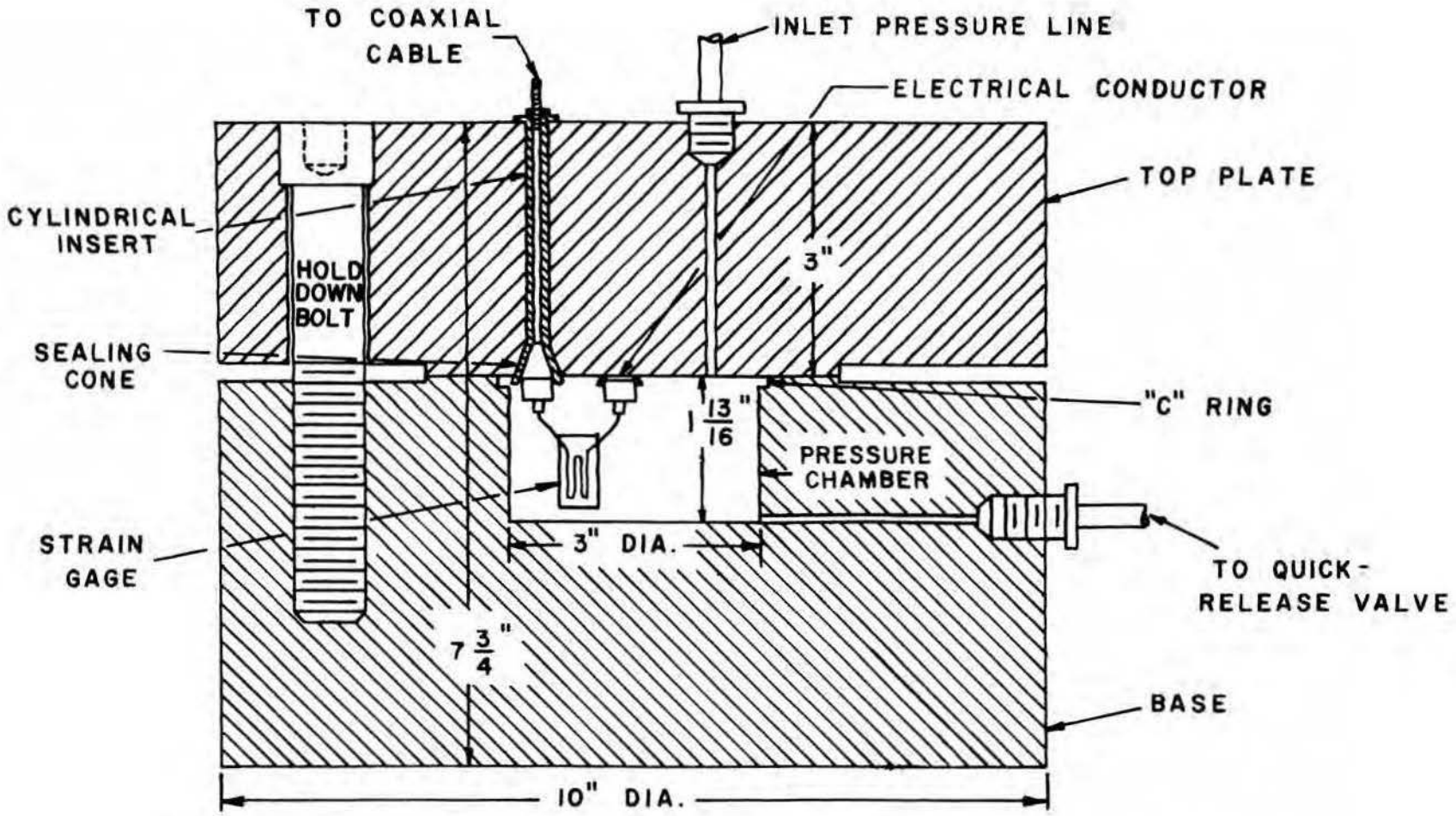

FIG. 1 CROSS-SECTIONAL VIEW OF PRESSURE POT

pressure pot to insure the existence of a proper pressure seal for the following runs.

Three SR-4 Budd strain-gages (gage factor 2.04±0.04) were mounted on copper cubes(0.12x1.00x0.53) which were placed in the chamber of the pressure pot. Three cubes were placed in the chamber so that failure of a gage would not necessitate removal of the top plate, but simply the use of another gage. The gages were mounted using Eastman-910 contact cement. The gage leads were soldered to the electrical conductors (Fig. 1), and then waterproofed by applying four thin coats of Budd GW-2 waterproofing compound to the gages, gage leads, and electrical connectors.

The pump was a single-ended vertical hand pump with a ½-gallon reservoir, with specifications as shown in Table I.

Table I - Hand Pump Specifications

Maximum Working Pressure	psi	40,000
Test Pressure	psi	50,000
Plunger Diameter	in	0.25
Working Stroke, nominal	in	1.00
Volume Displaced	in^3	0.80

The pump was connected to the pressure pot by use of standard ¼-inch O.D. by 1/16-inch I.D. high-pressure tubing.

2. INSTRUMENTATION

The instrumentation consisted of three components; (1) a Budd Strain Gage Bridge, (2) an oscilloscope and its various plug-in units, and (3) a triggering mechanism. Before proceeding, it should be noted that all components of the instrumentation were grounded and shielded cable was used

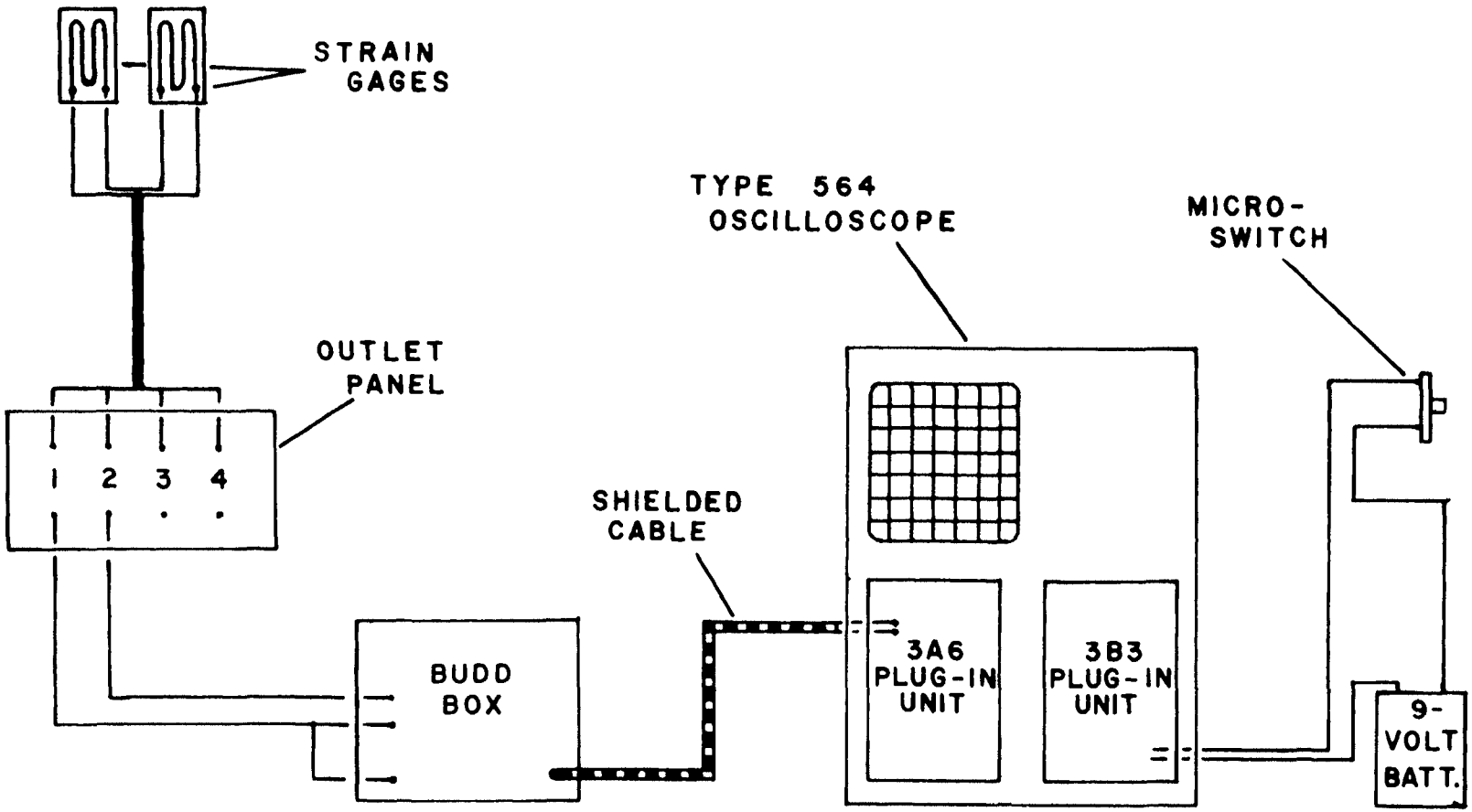

FIG. 2 INSTRUMENTATION COMPONENTS AND THE WORKING SET-UP

whenever possible to minimize external noise. Fig. 2 shows all components of the instrumentation and the working set-up.

The oscilloscope was a Type 564 manufactured by Tektronix Inc. which employed two plug-in units, a Type 3B3 Time Base Unit and a Type 3A6 Dual Trace Unit. A shielded cable connected the Budd Box and the 3A6 Dual Trace Amplifier Plug-In Unit (Fig. B-3). This unit is equipped with a two channel system, each containing a variable volts/division control. Only one channel (Channel 1) was used during the experimental work.

The triggering device consisted of a micro-switch mounted on the frame of the quick-release mechanism (Fig. B-4). The micro-switch was put in series with a common 9-volt battery and the 3B3 Time Base Plug-In Unit. This unit contains a variable time/division selector and the sweep triggering mechanism.

A Tektronix Camera System was mounted on the bezel of the oscilloscope (Fig. B-5). This system used Polaroid Land Pack Film that can be purchased commercially. A typical trace was obtained by first taking an exposure of the grid only, using a shutter speed of 1/5 of a second at f/4.5. The scale illumination was then turned completely off, the shutter set at open and the trace then triggered. The shutter was then closed and the picture developed.

3. QUICK-RELEASE MECHANISM

The quick-release mechanism consisted of a quick opening valve manufactured by American Instrument Company (Fig. B-4).

This valve is essentially a high-pressure valve held closed by a heavy spring. A metal disk was inserted in the spring in order to make contact and trigger the micro-switch. The spring was compressed by a cam fastened by a long-levered handle. The pressure release occurred when the spring was suddenly released, and took less than ten milliseconds for complete opening.

B. EXPERIMENTAL PROCEDURES

The experimental work was designed such that there existed three totally independent variables. They are: (1) length of the exit tube, (2) type of oil used, (3) initial pressure in the pressure pot.

There were three lengths of exit tubes, all standard high-pressure tubing. The lengths of the tubes were 36 inches, 72 inches, and 144 inches.

Two types of oil samples were used, one a paraffinic base oil and the other a naphthenic base oil. The properties of these oils are shown in Tables II and III.

The test runs were made by varying the initial pressure while using the same tube length and oil sample. A set of runs consisted of runs with initial pressures varying from 10,000 psi to 50,000 psi. Upon completion of a set of runs, a new tube length was added and a similiar set of runs made. After a set of runs was conducted for each tube length, the oil sample was changed and a set of runs for each tube length was made.

Table II - Viscosity and Density Data

OIL SAMPLE	R-820-53 (PARAFFINIC)	R-820-54 (NAPHTHENIC)
Kinematic Viscosity/210° F (cst)	5.400	3.654
Kinematic Viscosity/100° F (cst)	33.740	22.620
Viscosity Index	103	6
Density at 100° F	0.850	0.895
Density at 210° F	0.810	0.855

Table III - Volume at Pressure and Temperature

	VOLUME (IN^3)			
	PARAFFINIC		NAPHTHENIC	
Temperature (°F)	100	200	100	200
Pressure (ksi)				
0	1.176	1.235	1.117	1.170
5	1.152	1.202	1.096	1.141
10	1.133	1.176	1.079	1.119
15	1.116	1.155	1.064	1.101
20	1.102	1.138	1.051	1.085
30	1.078	1.110	1.030	1.059
40	1.059	1.096	1.012	1.039
50	1.042	1.069	0.997	1.021
60	1.028	1.053	0.984	1.006

C. EXPERIMENTAL RESULTS

A total of forty test runs were made, twenty-seven using paraffinic base oil and thirteen using naphthenic base oil. A list of these tests is presented in Table IV.

Typical pressure-time traces within the pressure pot are illustrated in Fig. B-6 to B-11. It should be noted that all traces were quite similar. In each instance, the pressure began to decline exponentially, then leveled off for several milliseconds before continuing its exponential decay. The traces obtained by Dr. R.L. Davis (Ref. c) decayed exponentially with no plateau or leveling off occurring (Fig. B-12 and B-13); however, a different release mechanism was used by Dr. Davis. His release mechanism was a knock-off tube exposed directly to the atmosphere (Fig. 3a) whereas with the quick-release valve the oil had to exit at a right angle (Fig. 3b).

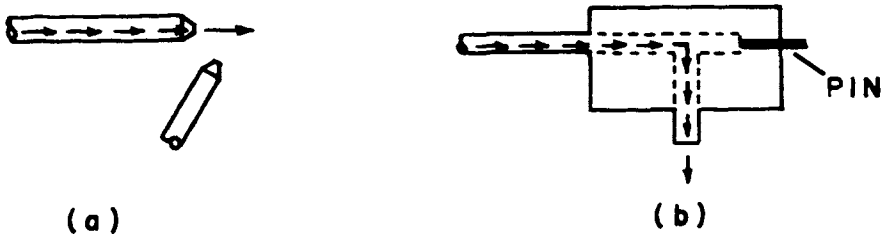

FIG. 3 TYPES OF RELEASE MECHANISMS

As the pin released in the quick-release mechanism, it reacted as a piston receding from the fluid; thus, suggesting a rarefaction wave had occurred.

Table IV - Control Data

RUN NO.	OIL SAMPLE*	TUBE LENGTH** (IN)	VOLTS/DIV.	TIME/DIV. (MSEC)	INITIAL PRESS. (PSI)
1	1	1	.01	5	10,000
2	1	1	.01	10	20,000
3	1	1	.01	10	25,000
4	1	1	.02	10	30,000
5	1	1	.05	10	35,000
6	1	1	.05	10	40,000
7	1	1	.05	10	45,000
8	1	1	.10	10	50,000
9	1	2	.20	10	10,000
10	1	2	.20	10	20,000
11	1	2	.20	10	25,000
12	1	2	.20	10	30,000
13	1	2	.20	10	35,000
14	1	2	.20	10	40,000
15	1	2	.20	10	45,000
16	1	2	.20	10	50,000
17	1	3	.10	10	10,000
18	1	3	.20	10	20,000
19	1	3	.20	10	25,000
20	1	3	.20	10	30,000
21	1	3	.20	10	35,000
22	1	3	.20	10	40,000
23	1	3	.20	10	45,000
24	1	3	.20	10	50,000
8A	1	1	.20	10	50,000

* OIL SAMPLE
1 - Paraffinic Base Oil
2 - Naphthenic Base Oil

** TUBE LENGTH
1--36 inches
2--72 inches
3--144 inches

Table IV - Control Data (Cont.)

RUN NO.	OIL SAMPLE*	TUBE LENGTH** (IN)	VOLTS/DIV.	TIME/DIV. (MSEC)	INITIAL PRESS. (PSI)
8B	1	1	.20	20	50,000
6A	1	1	.20	20	40,000
25	2	1	.10	10	20,000
26	2	1	.20	20	30,000
27	2	1	.20	20	40,000
28	2	1	.20	20	45,000
29	2	2	.20	20	30,000
30	2	2	.20	20	30,000
31	2	2	.20	20	20,000
32	2	2	.20	20	30,000
33	2	2	.20	20	40,000
34	2	3	.20	20	20,000
35	2	3	.20	20	30,000
36	2	3	.20	20	40,000
37	2	3	.20	20	10,000

By expressing the pressure as a power series function of the density ($P= a_o+a_1\rho+a_2\rho^2+a_3\rho^3$), and solving simultaneous equations obtained by substitution of known densities at various pressures, the following data was tabulated using the wave equations given in references (g) and (h)

Table V - Rarefaction Wave Data
(Paraffinic Base Oil)

		Tube Length		
		36"	72"	144"
Pressure (ksi)	Velocity (in/sec)	Time to travel length of tube (msec)		
20	2,315	15.6	31.1	62.2
40	2,231	16.1	32.3	64.5

Figure B-6, which is a trace of the Paraffinic Base Oil under an initial pressure of 40,000 psi, shows that for a 36" tube length the time for a wave to affect the exponential decay of the pressure is approximately 15 msec, which compares quite favorably with the 16.6 msec from Table V. Since a rarefaction wave acts as a signal transmitter, this suggests the possibility of a compression wave initiated by the rebounding of the release pin. This would also explain why no plateau or leveling-off was evident when the knock-off tube was used.

III. ANALYTICAL EFFORTS

A. CLOSED-FORM SOLUTION

Several assumptions were made at the beginning of the problem: (1) the working temperature was constant, (2) laminar flow existed along the length of the tube, (3) the quick-release valve opened instantaneously, and (4) there were no turbulent effects at the entrance of the tube. The analysis commences with a general expression for the equation of motion of a viscous, compressible fluid expressed in vector form (Ref. c) as

$$\rho \frac{d\bar{v}}{dt} = \rho \bar{F} - \nabla P - \frac{2}{3} \nabla \left[\mu (\nabla \cdot \bar{v}) \right] + \left[\nabla \cdot (2\mu \nabla) \right] \bar{v} + \nabla \times (\mu \bar{\xi}) \tag{1}$$

where the vorticity vector $\bar{\xi}$ is defined as

$$\bar{\xi} = \nabla \times \bar{v} \tag{2}$$

Combining equations (1) and (2) and simplifying yields

$$\rho \frac{d\bar{v}}{dt} = \rho \bar{F} - \nabla P + \frac{1}{3} \mu \nabla (\nabla \cdot \bar{v}) - \frac{2}{3} \nabla \mu (\nabla \cdot \bar{v}) + \mu (\nabla \cdot \nabla) \bar{v} + 2 \left[\nabla \mu \cdot \nabla \right] \bar{v} + \nabla \mu \times \bar{\xi} - \mu \nabla \times \bar{\xi} \tag{3}$$

The addition of the viscosity term alters the essential nature of the partial differential equation in that it has the highest derivative. Compressibility on the other hand, adds only low order derivatives(Ref. g). Thus the condition of incompressibility was assumed.

Assuming the condition of incompressibility and considering the coefficient of viscosity to be independent of spatial

coordinates, equation (3) reduces to

$$\rho \frac{d\bar{v}}{dt} = \rho F - \nabla P - \mu \nabla \times \bar{\xi}$$

or

$$\frac{d\bar{v}}{dt} = \bar{F} - \frac{1}{\rho} \nabla P + \nu \nabla^2 \bar{v} \tag{4}$$

where

$$\nu = \frac{\mu}{\rho} \tag{5}$$

Expanding equation (4) into its components in cylindrical coordinates yields the Navier-Stokes equations for a viscous, incompressible fluid

$$\frac{\partial u}{\partial t} + u\frac{\partial u}{\partial r} + \frac{v}{r}\frac{\partial u}{\partial \theta_1} + w\frac{\partial u}{\partial z} - \frac{v^2}{r} = F_1 - \frac{1}{\rho}\frac{\partial P}{\partial r} + \nu\left(\frac{\partial^2 u}{\partial r^2} + \frac{1}{r}\frac{\partial u}{\partial r} + \frac{1}{r^2}\frac{\partial^2 u}{\partial \theta_1^2} - \frac{u}{r^2} - \frac{2}{r^2}\frac{\partial v}{\partial \theta_1} + \frac{\partial^2 u}{\partial z^2}\right) \tag{6a}$$

$$\frac{\partial v}{\partial t} + u\frac{\partial v}{\partial r} + \frac{v}{r}\frac{\partial v}{\partial \theta_1} + w\frac{\partial v}{\partial z} - \frac{uv}{r} = F_2 - \frac{1}{\rho r}\frac{\partial P}{\partial \theta_1} + \nu\left(\frac{\partial^2 v}{\partial r^2} + \frac{1}{r}\frac{\partial v}{\partial r} + \frac{1}{r^2}\frac{\partial^2 v}{\partial \theta_1^2} - \frac{v}{r^2} + \frac{2}{r^2}\frac{\partial u}{\partial \theta_1} + \frac{\partial^2 v}{\partial z^2}\right) \tag{6b}$$

$$\frac{\partial w}{\partial t} + u\frac{\partial w}{\partial r} + \frac{v}{r}\frac{\partial w}{\partial \theta_1} + w\frac{\partial w}{\partial z} = F_3 - \frac{1}{\rho r}\frac{\partial P}{\partial z} + \nu\left(\frac{\partial^2 w}{\partial r^2} + \frac{1}{r}\frac{\partial w}{\partial r} + \frac{1}{r^2}\frac{\partial^2 w}{\partial \theta_1^2} + \frac{\partial^2 w}{\partial z^2}\right) \tag{6c}$$

If the conditions of constant temperature, negligible body forces per unit mass, and constant density are now invoked, and assuming the fluid flow is in the z-direction only, equations (6) reduce to

$$\frac{\partial w}{\partial t} = -\frac{1}{\rho}\frac{\partial P}{\partial z} + \nu\left(\frac{\partial^2 w}{\partial r^2} + \frac{1}{r}\frac{\partial w}{\partial r}\right) \qquad (7)$$

From reference (b), the pressure along the longitudinal axis of the tube is considered to vary linearly from the maximum value at the chamber entrance to atmospheric pressure at the end of the tube (Fig. 4).

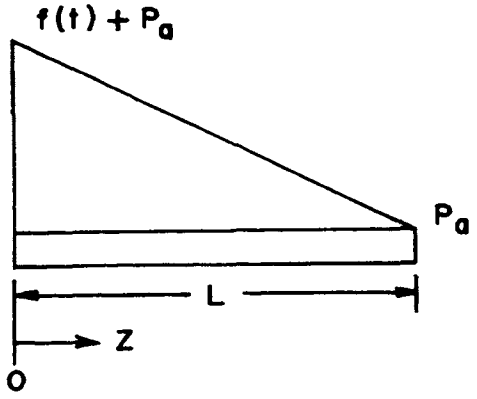

FIG. 4 PRESSURE DECAY WITHIN TUBE

The pressure within the tube can be expressed in terms of time and the z-coordinate as

$$P = f(t)\left[1 - \frac{z}{L}\right] + P_A \qquad (8)$$

where f(t) is the pressure within the pressure pot and is a function of time only. Differentiation of both sides of equation (8) with respect to z yields

$$\frac{\partial P}{\partial z} = -\frac{f(t)}{L} \qquad (9)$$

Substitution of equation (9) into equation (7) yields

$$\nu\left(\frac{\partial^2 w}{\partial r^2} + \frac{1}{r}\frac{\partial w}{\partial r}\right) - \frac{\partial w}{\partial t} = -\frac{f(t)}{\rho L} \qquad (10)$$

According to Hersey in reference (d) and Weiner in reference (e), the kinematic viscosity can be closely approximated in the pressure range of 0 psi to 50,000 psi by the relation

$$\nu = \nu_o e^{m f(t)} \qquad (11)$$

where ν_o = kinematic viscosity under atmospheric pressure
m = slope of log viscosity-pressure curve

Equation (10) can now be written

$$\nu_o e^{mf(t)}\left(\frac{\partial^2 w}{\partial r^2} + \frac{1}{r}\frac{\partial w}{\partial r}\right) - \frac{\partial w}{\partial t} = -\frac{f(t)}{\rho L} \qquad (12)$$

The boundary condition

$$w(R_o, t) = 0 \qquad t \geq 0 \qquad (13)$$

and initial condition

$$w(r, 0) = 0 \qquad 0 < r < R_o \qquad (14)$$

defines a unique solution to equation (12).

The homogeneous solution of equation (12) is found by using separation of variables

$$w_H(r, t) = R(r)\,T(t) \qquad (15)$$

to be

$$w_H(r,t) = \sum_{j=1}^{\infty} C_j J_0(\lambda_j r) \left\{ e^{\lambda_j \nu \theta} \left[\ln (mf(t)) + mf(t) + \frac{1}{2 \cdot 2!}(mf(t))^2 + \cdots\cdots + \frac{1}{n \cdot n!}(mf(t))^n \right] \right\} \tag{16}$$

Before proceeding, a proper choice of f(t) must be made. The choice of

$$f(t) = P_g e^{-t/\theta} \tag{17}$$

is suggested from an observation of pressure time traces monitored in the pressure pot. In order to illustrate possible solutions of the governing differential equation, the assumption of constant viscosity (m=0) is invoked. Equation (10) thus becomes

$$\nu \left(\frac{\partial^2 w}{\partial r^2} + \frac{1}{r} \frac{\partial w}{\partial r} \right) - \frac{\partial w}{\partial t} = - \frac{P_g}{\rho L} e^{-t/\theta} \tag{18}$$

The homogeneous solution given in equation (16) can be added to the particular solution of equation (18), subject to the restrictions specified in equation (13) and (14), to give

$$w(r,t) = \frac{2 P_g}{\rho L R_0} \sum_{j=1}^{\infty} \frac{J_0(\lambda_j r)}{\lambda_j J_1(\lambda_j R_0)} \left[\frac{1}{1/\theta - \nu \lambda_j^2} \right] \left[e^{-\lambda_j \nu t} - e^{-t/\theta} \right] \tag{19}$$

Calculating the volume rate of fluid Q passing through the tube in time t, we get

$$Q = \int_0^A w(r,t)\, da \tag{20}$$

or

$$Q = \frac{4\pi P_g}{\rho L} \sum_{j=1}^{\infty} \left[\frac{1}{1/\theta - \nu \lambda_j^2} \right] \left[e^{-\lambda_j^2 \nu t} - e^{-t/\theta} \right] \left[\frac{1}{\lambda_j^2} \right] \tag{21}$$

The volume of fluid that must exit the chamber during depressurization is calculated by the equation

$$V_o = \int_0^\infty Q\,dt \tag{22}$$

which when integrated and simplified becomes

$$V_o = \frac{4\pi P_g \theta}{\mu L} \sum_{j=1}^{\infty} \frac{1}{\lambda_j^4} \tag{23}$$

The coefficients λ_j were defined as the roots of the equation

$$J_0(\lambda_j R_0) = 0 \tag{24}$$

in order that the boundary conditions equation (13) be identically satisfied. Thus, equation (23) can now be written as

$$V_o = \frac{\pi \theta P_g R^4}{8\mu L} \tag{25}$$

From reference (f), the compressibility of the fluid can be approximated by the equation

$$\frac{V_1}{V_2} = 1.0 - (4.31\times10^{-6})P_g + (6.51\times10^{-11})P_g^2 - (5.03\times10^{-16})P_g^3 \tag{26}$$

where V_1 = volume of fluid under pressure P_g
V_2 = volume of fluid under atmospheric pressure

Since $V_o = V_2 - V_1$

$$V_o = V_1 P_g K_p \tag{27}$$

where the fluid compressibility factor is

$$K_p = \left[\frac{4.31\times10^{-6} - (6.5\times10^{-11})P_g + (5.03\times10^{-16})P_g^2}{1.0 - (4.31\times10^{-6})P_g + (6.51\times10^{-11})P_g^2 - (5.03\times10^{-16})P_g^3}\right]$$

Thus, the time constant θ can be expressed as

$$\theta = \frac{8\mu L V_1 K_p}{\pi R_o^4} \tag{28}$$

Once the system parameters μ, L, V, K_p, and R_o are given, equation (28) defines the time constant θ that, when used with equation (17), determines the pressure decay in a pressure pot that is instantly exposed to the atmosphere via a circular tube. The corresponding flow characteristics in the circular tube are described by the velocity profiles, equation (19), and the volume flow rate, equation (21). It should be noted that the application of equation (28) is limited to fluids that are insensitive to pressure environments, or to pressure levels that create small changes in the fluid viscosity. Experimentation has indicated that, for the subject fluids, equation (28) is invalid for pressures in excess of 10,000 psi.

Using the choice of f(t) described in equation (17) in the equation for variable viscosity, equation (11), and then substituting into equation (18) yields

$$\nu_o e^{mP_g e^{-t/\theta}} \left(\frac{\partial^2 w}{\partial r^2} + \frac{1}{r} \frac{\partial w}{\partial r} \right) - \frac{\partial w}{\partial t} = -\frac{P_g}{\rho L} e^{-t/\theta} \tag{29}$$

The homogeneous solution found in equation (16) again applies to equation (29), thus

$$w_H(r,t) = \sum_{j=1}^{\infty} C_j J_o(\lambda_j r) \left\{ e^{\lambda_j \nu \theta} \left[\ln(mP_g e^{-t/\theta}) + mP_g e^{-t/\theta} + \frac{1}{2 \cdot 2!}(mP e^{-t/\theta})^2 + \cdots + \frac{1}{n \cdot n!}(mP e^{-t/\theta})^n \right] \right\} \tag{30}$$

If a particular solution can now be found, the definition of

the time constant using the assumption of variable viscosity will be completed. A probable choice of a particular solution is

$$w_p(r,t) = A e^{-t/\theta} \tag{31}$$

which upon substitution into equation (29) yields

$$-\left(-\frac{A}{\theta} e^{-t/\theta}\right) = -\frac{P_g}{\rho L} e^{-t/\theta} \tag{32}$$

Solving for A

$$A = -\frac{\theta P_g}{\rho L}$$

and substituting into equation (31) gives

$$w_p(r,t) = -\frac{\theta P_g}{\rho L} e^{-t/\theta} \tag{33}$$

The solution of equation (29) can now be written as the sum of the homogeneous and particular solutions

$$w(r,t) = \sum_{j=1}^{\infty} C_j J(\lambda_j r)\left\{e^{\lambda_j^2 \nu \theta}\left[\ln(mP_g e^{-t/\theta}) + mP_g e^{-t/\theta} + \frac{1}{2\cdot 2!}(mP_g e^{-t/\theta})^2 + \cdots + \frac{1}{n\cdot n!}(mP_g e^{-t/\theta})^n\right]\right\} - \frac{\theta P}{\rho L} e^{-t/\theta} \tag{34}$$

Since the constants C_j and λ_j must be such that equations (13) and (14) are satisfied, equation (34) is rewritten as

$$w(r,t) = \sum_{j=1}^{\infty} C_j J_0(\lambda_j r)\left\{e^z - g(t)\right\} \tag{35}$$

where

$$z = \lambda_j^2 \nu_o \theta\left[\ln(mP_g e^{-t/\theta}) + mP_g e^{-t/\theta} + \frac{1}{2\cdot 2!}(mP_g e^{-t/\theta})^2 + \cdots + \frac{1}{n\cdot n!}(mP_g e^{-t/\theta})^n\right]$$

Noting that the Bessel function $J_o(\lambda_j r)$ is the only function of r, substitution of equation (35) into equation (12) and simplifying yields

$$\sum_{j=1}^{\infty} C_j J(\lambda_j r)\left\{\lambda_j^2 \nu_o e^{mP_g e^{-t/\theta}} g(t) + g'(t)\right\} = -\frac{P_g}{\rho L} e^{-t/\theta} \qquad (36)$$

If the equation

$$\lambda_j^2 \nu_o e^{mP_g e^{-t/\theta}} g(t) + g'(t) = e^{-t/\theta} \qquad (37)$$

can be solved for g(t), the constants C_j are given according to the Fourier-Bessel expansion as

$$C_j = -\frac{\frac{P_g}{\rho L}\int_0^{R_o} r\, J_o(\lambda_j r)\, dr}{\frac{1}{2}R_o^2\left[J_o^2(\lambda_j r) + J_1^2(\lambda_j R_o)\right]} \qquad (38)$$

Equation (13) is satisfied if λ_j is defined as the positive roots of the equation

$$J_o(\lambda_j R_o) = 0 \qquad (39)$$

Thus equation (38) becomes

$$C_j = -\frac{2P_g}{\rho L R_o \lambda_j}\left[\frac{1}{J_1(\lambda_j R_o)}\right] \qquad (40)$$

Numerous attempts to solve equation (37) with the initial condition given by equation (14) were made, among them substitution methods, integration by parts, series solution, and numerical means and methods. One such closed-form attempt began with the assumption that

$$g(t) = h(t)\, e^{y} \qquad (41)$$

where

$$y = \ln\left(mP_g e^{-t/\theta}\right) + mP_g e^{-t/\theta} + \frac{1}{2\cdot 2!}\left(mP_g e^{-t/\theta}\right)^2$$

$$+ \cdots\cdots + \frac{1}{n\cdot n!}\left(mP_g e^{-t/\theta}\right)^n$$

Equation (41) was chosen because of the fact that when it is combined with equation (37) the following, less complex equation is obtained

$$h'(t)e^{y} = e^{-t/\theta} \tag{42}$$

Integrating both sides gives

$$h(t) = \int e^{-y}e^{-t/\theta}dt \tag{43}$$

Integration by parts failed to solve equation (43). The application of numerical techniques could be used to solve equation (43); however, if numerical schemes are to be employed, they can be applied more efficiently elsewhere in the program as explained in the following section.

B. NUMERICAL ANALYSIS

The numerical analysis was based on the constant viscosity closed-form solution. A series of constant pressure increments was used to simulate the pressure-time trace shown in Fig. 5.

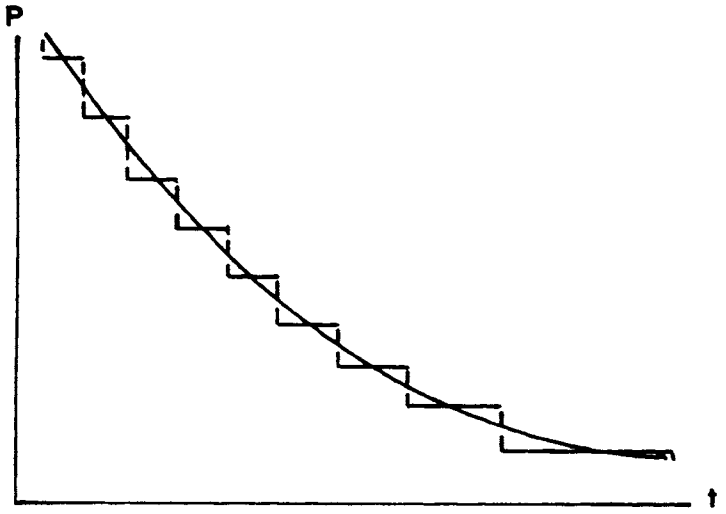

FIG. 5 PRESSURE - TIME TRACE

Each increment, or step, of time is assumed to have constant viscosity. Thus the working equation for each step is

$$\nu \left(\frac{\partial^2 w}{\partial r^2} + \frac{1}{r} \frac{\partial w}{\partial r} \right) - \frac{\partial w}{\partial t} = - \frac{P_g}{\rho L} e^{-t/\theta} \qquad (18)$$

the solution of which is

$$w(r,t) = \frac{2 P_g}{\rho L R_o} \sum_{j=1}^{\infty} \frac{J_o(\lambda_j r)}{\lambda_j J_1(\lambda_j R_o)} \left[\frac{1}{1/\theta - \nu \lambda_j^2} \right] \left[e^{-\lambda_j \nu t} - e^{-t/\theta} \right] \qquad (19)$$

For every increment of pressure, the viscosity and theta were calculated for eleven radial positions, beginning at the center-line and progressing out to the edge of the tube.

The program began by reading system parameters into the program (Appendix A) in steps 3 to 11(See Fig. 7). Arg (1)

in step 10 is the first solution of the equation

$$J_0(\lambda_j R_0) = 0 \qquad (39)$$

and subsequent solutions to the equation were calculated as needed in step 47. The R(1) in step 11 is the radius at the center line. The radius was made dimensionless by forming the quotient r/R_o and broken into increments of 0.1 as needed by step 42.

The fluid compressibility factor K_p (equation 27) was calculated in steps 16-18. The pressure was next incremented depending on the present value of the pressure. Since the pressure decay in the pressure pot was exponential (Fig. 6)

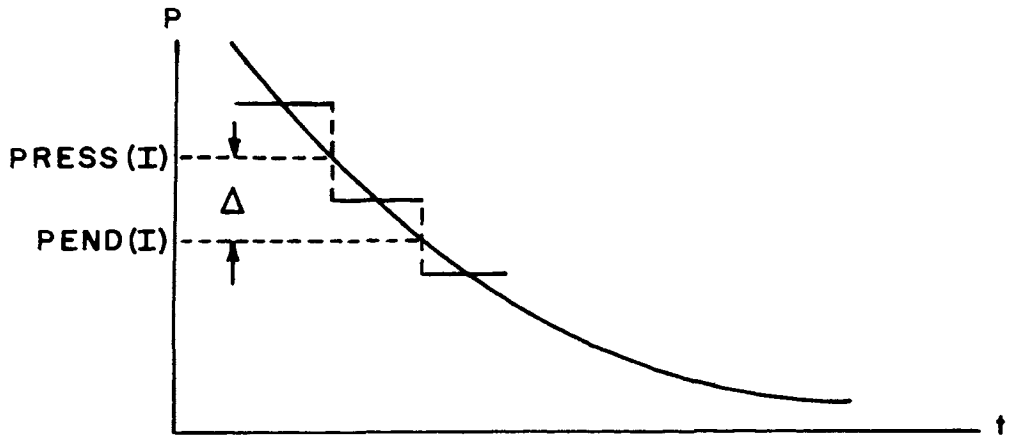

FIG. 6 INCREMENT OF PRESSURE-TIME TRACE

a smaller increment of pressure was necessitated at the beginning of the run due to the greater slope. The pressure at the end of the increment was calculated by subtracting the increment size from the pressure at the beginning of the increment. The average pressure, $\text{press}(I)-\frac{\Delta}{2}$, was used in all calculations involving variable pressure.

The viscosity of the various increments was calculated in step 36 using equation (11). The time constant theta was next calculated by use of equation (28). Rewriting equation (17) as

$$f(t) = P \tag{44}$$

yields

$$t = -\theta \ln \frac{P}{P_g} \tag{45}$$

which enables the calculation of the time length of the various increments in step 39.

The terms PROD1(K) and PROD2(K) are terms common to equations (19) and (21). Steps 52 through 68 were series calculations of the Bessel Functions of the first and second order (Ref. a). The velocities, w(r,t), volume rate of fluid flow, Q, and the volume of fluid, V, were calculated in steps 74 to 76 using equations (19), (21), and (23) respectively.

The pressure was now incremented in step 79 by equating PRESS (I+1)=PEND(I), and the program was then returned to step 19. This looping process continued until PEND(I)$\leq$0, at which time the program was terminated.

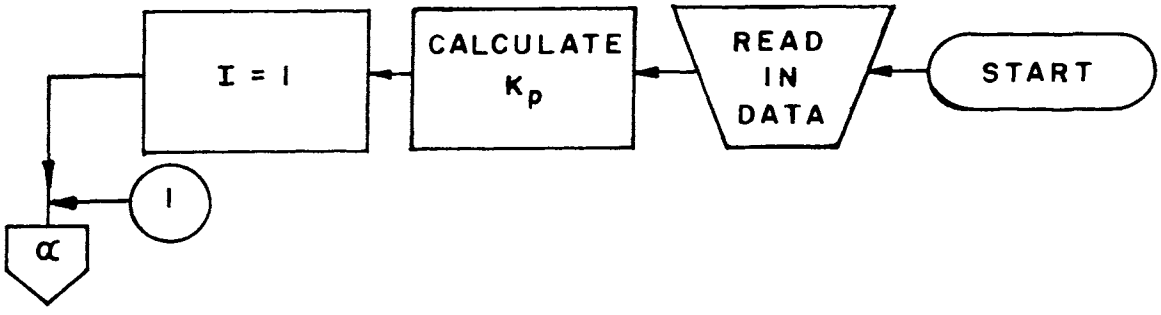

FIG. 7 - FLOW CHART

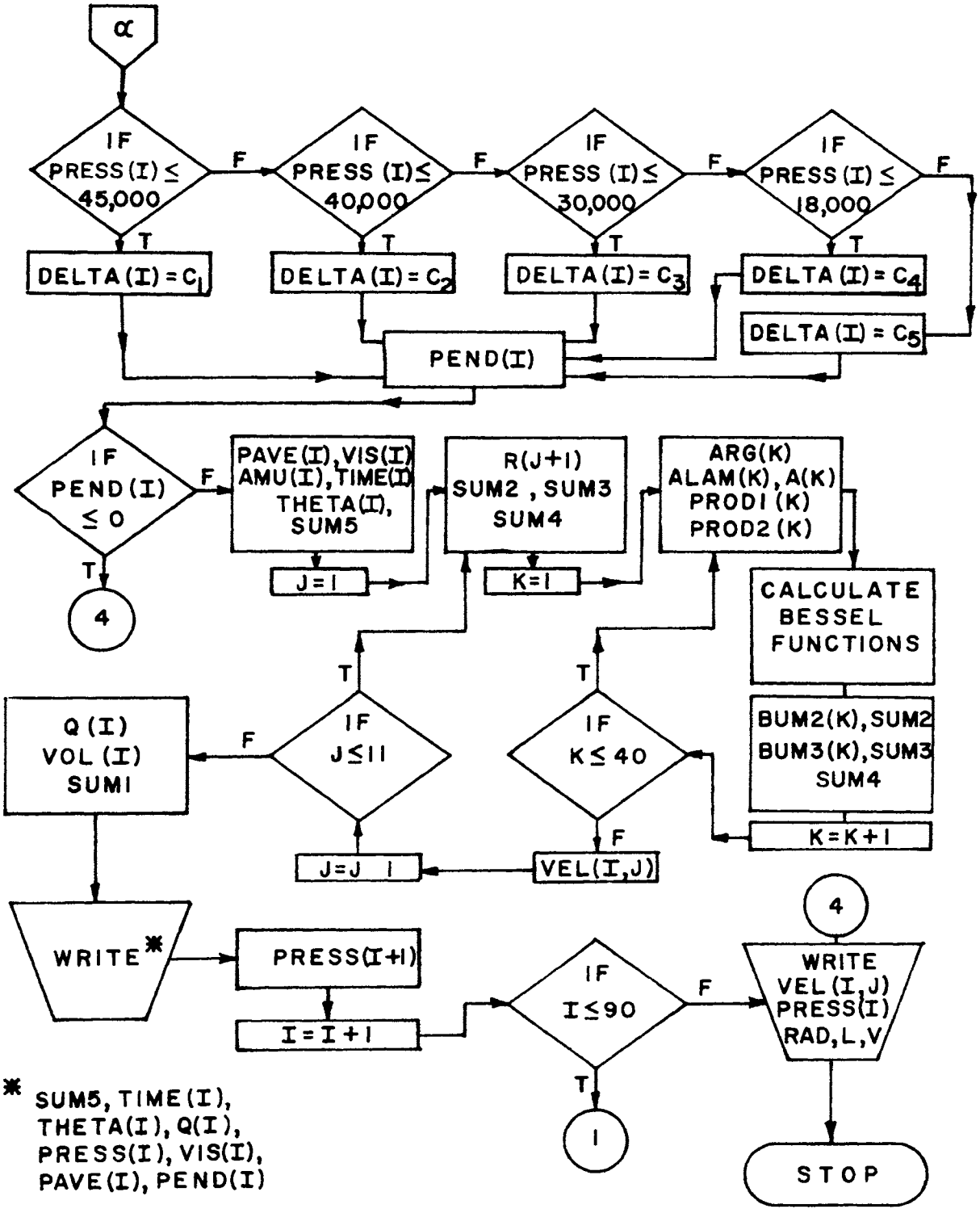

FIG. 7 - FLOW CHART (CONT.)

C. NUMERICAL RESULTS

The results of the computer program are shown by the traces or graphs in Appendix C. Figure C-1 shows the decay of pressure in the pressure pot with respect to time. Since the pressure was assumed to decay exponentially over each increment, it could be expected that Figure C-1 would also represent an exponential decay. The kinematic viscosity-pressure trace shown in Figure C-2 consists of data from all the runs overlapped and only one trace was therefore obtained. In the remaining traces, constant viscosity refers to traces obtained using the closed-form solution (Eq. 19) and variable viscosity refers to traces obtained from program data. Figures C-3 and C-4. both velocity profile traces, are representative of typical profiles for constant and variable viscosities, respectively. The next four traces, Figure C-5 through C-8, are comparisons of velocity profiles for constant and variable viscosities for given pressures. The final graph compares the velocity-time history at the tube centerline for the two viscosity conditions.

IV. SUMMARY AND CONCLUSIONS

The closed-form solution, obtained in equation (19) by assuming the fluid viscosity to be constant, was used for the formulation of the computer program that would solve the pressure-induced variable viscosity flow problem. The computer program yielded good results for the velocity profiles, pressure-time, velocity-time, and kinematic viscosity-pressure traces. The magnitudes of the velocities were lower than those obtained by the constant viscosity solution in all cases. No correlation was anticipated for the initial pressures of approximately 10,000 psi and above. This is expected since the constant viscosity solution was shown in reference (c) to be acceptable for pressures of approximately 10,000 psi and below. Although the velocities become closer as the pressure decreases, the large differences that exist at the high pressure levels certainly dictate that the effect of pressure on the fluid viscosity must be included in the analysis.

The experimental traces differed from those in reference (c) by the fact of a plateau or leveling-off. This difference was explained by the use of the quick-release mechanism instead of the knock-off tubes. The right angle of exit produced a rarefaction wave which transversed back down the tube, thus causing a plateau to show on the traces.

In conclusion, the computer solution presented in this report yielded favorable results for the study of the flow

of a variable viscosity fluid through a circular duct with direct exposure to the atmosphere. Although ordinary pressures are not usually considered to influence the fluid viscosity, and hence the flow characteristics, for the particular problem investigated, the effects of pressure play a dominant role and cannot be neglected.

V. APPENDICES

APPENDIX A. COMPUTER PROGRAM

```
/WAT4  FM120262,TIME=12,PAGES=010          WEBER                              JOB
C      FINITE DIFFERENCE ANALYSIS OF VARIABLE VISCOSITY FLUID FLOW
C      THROUGH CIRCULAR DUCTS
C      DEFINITION OF TERMS
C        PRESS(I)    PRESSURE AT START OF INCREMENT        LB/IN**2
C        PEND(I)     PRESSURE AT END OF INCREMENT          LB/IN**2
C        PAVE(I)     AVERAGE PRESSURE OF INCREMENT         LB/IN**2
C        RHO         MASS DENSITY OF FLUID                 LB-SEC**2/IN**4
C        AM          SLOPE OF PRESSURE-VSICOSITY CURVE     IN**2/LB
C        L           BORE LENGTH                           IN
C        V           CHAMBER VOLUMN                        IN**3
C        RAD         INSIDE RADIUS OF TUBE                 IN
C        VIS(I)      KINEMATIC VISCOSITY                   IN**2/SEC
C        AMU(I)      COEFFICIENT OF VISCOSITY              LB-SEC/IN**2
C        THETA(I)    TIME CONSTANT OF PRESSURE RELEASE     SEC
C        VEL(I,J)    VELOCITY                              IN/SEC
C        Q(I)        VOLUMN RATE OF FLUID FLOW             IN**3/SEC
C        VOL(I)      VOLUMN OF FLUID FLOW                  IN**3
      1  DIMENSION PRESS(92),PEND(92),PAVE(92),VIS(92),AMU(92),THETA(92),
     1TIME(92),R(42),ARG(42),ALAM(42),A(42),PROD1(42),PROD2(42),
     2W(42),B(42),G(42),H(42),S(42),X(42),C(42),T(42),SUM2(42),SUM3(42),
     3VEL(92,92),Q(92),VOL(92),DELTA(92)
      2  REAL L
      3  RHO=7.72E-5
      4  AM=5.30E-5
      5  L=5.00
      6  V=12.80
      7  RAD=3.125E-2
      8  PI=3.14
      9  PRESS(1)=14900.0
     10  ARG(1)=2.4048
     11  R(1)=0.00
     12  SUM1=0.00
     13  SUM5=0.00
     14  KK=1
     15  WRITE(3,100)
     16  COMP1=4.31E-6-(6.51E-11*PRESS(1))+(5.03E-16*(PRESS(1)**2))
     17  COMP2=1.0-(4.31E-6*PRESS(1))+(6.51E-11*(PRESS(1)**2))-(5.03E-16
     1*(PRESS(1)**3))
```

```
      COMP=COMP1/COMP2
      DO 10 I=1,90
      IF(PRESS(I)-45000.0)2,2,1
    1 DELTA(I)=50.0
      GO TO 20
    2 IF(PRESS(I)-40000.0)4,4,3
    3 DELTA(I)=100.0
      GO TO 20
    4 IF(PRESS(I)-30000.0)6,6,5
    5 DELTA(I)=100.0
      GO TO 20
    6 IF(PRESS(I)-18000.0)8,8,7
    7 DELTA(I)=100.0
      GO TO 20
    8 DELTA(I)=100.0
   20 PEND(I)=PRESS(I)-DELTA(I)
      IF(PEND(I)-0.0)30,30,9
    9 PAVE(I)=PRESS(I)-(DELTA(I)/2.0)
      VIS(I)=12.77E-2*EXP(AM*PAVE(I))
      AMU(I)=VIS(I)*RHO
      THETA(I)=(8.0*L*V*COMP*AMU(I))/(PI*RAD**4)
      TIME(I)=-THETA(I)*ALOG(PEND(I)/PRESS(I))
      SUM5=SUM5+TIME(I)
      DO 40 J=1,11
      R(J+1)=R(J)+(RAD/10.0)
      SUM2=0.0
      SUM3=0.0
      SUM4=0.0
      DO 50 K=1,40
      ARG(K+1)=ARG(K)+PI
      ALAM(K)=ARG(K)/RAD
      A(K)=R(J)*ALAM(K)
      PROD1(K)=THETA(I)/(1.0-THETA(I)*VIS(I)*ALAM(K)*ALAM(K))
      PROD2(K)=EXP(-VIS(I)*SUM5*ALAM(K)*ALAM(K))
     1-EXP(-SUM5/THETA(I))
      IF(A(K)-3.0)21,21,22
   21 W(K)=A(K)/3.0
      B(K)=1.0-2.2499997*(W(K)**2)+1.2656208*(W(K)**4)-0.3163866*
     1(W(K)**6)+0.0444479*(W(K)**8)-0.0039444*(W(K)**10)+0.0002100*
     2(W(K)**12)
      GO TO 60
   22 W(K)=3.0/A(K)
      G(K)=0.79788456-0.00000077*(W(K))-0.00552740*(W(K)**2)
     1-0.00009512*(W(K)**3)+0.00137237*(W(K)**4)-0.00072805*(W(K)**5)
     2+0.00014476*(W(K)**6)
```

```
      H(K)=A(K)-0.78539816-0.04166397*W(K)-0.00003954*(W(K)**2)
     1+0.00262573*(W(K)**3)-0.00054125*(W(K)**4)-0.00029333*(W(K)**5)
     2+0.00013558*(W(K)**6)
      B(K)=(G(K)*COS(H(K)))/SQRT(A(K))
   60 IF(ARG(K)-3.0)23,23,24
   23 S(K)=ARG(K)/3.0
      X(K)=0.500-0.56249985*(S(K)**2)+0.21093573*(S(K)**4)-0.03954289*
     1(S(K)**6)+0.00443319*(S(K)**8)-0.00031761*(S(K)**10)+0.00011109*
     2(S(K)**12)
      C(K)=X(K)*ARG(K)
      GO TO 70
   24 S(K)=3.0/ARG(K)
      T(K)=0.79788456+0.00000156*S(K)+0.01659667*(S(K)**2)+0.00017105*
     1(S(K)**3)-0.00249511*(S(K)**4)+0.00113653*(S(K)**5)-0.00020033*
     2(S(K)**6)
      X(K)=ARG(K)-2.35619449+0.12499612*S(K)+0.00005650*(S(K)**2)
     1-0.00637879*(S(K)**3)+0.00074348*(S(K)**4)+0.00079824*(S(K)**5)
     2-0.00029166*(S(K)**6)
      C(K)=(T(K)*COS(X(K)))/SQRT(ARG(K))
   70 BUM2(K)=(B(K)*PROD1(K)*PROD2(K))/(ALAM(K)*C(K))
      SUM2=SUM2+BUM2(K)
      BUM3(K)=(PROD1(K)*PROD2(K))/(ALAM(K)**2)
      SUM3=SUM3+BUM3(K)
   50 SUM4=SUM4+(1.0/(ALAM(K)**4))
   40 VEL(I,J)=(2.0*PRESS(I)*SUM2)/(RHO*L*RAD)
      Q(I)=(4.0*PI*PRESS(I)*SUM3)/(RHO*L)
      VOL(I)=(4.0*PI*PRESS(I)*THETA(I)*SUM4)/(AMU(I)*L)
      SUM1=SUM1+VOL(I)
      WRITE(3,200) SUM5,TIME(I),THETA(I),PRESS(I),PAVE(I),PEND(I),
     1Q(I),VIS(I)
      PRESS(I+1)=PEND(I)
   10 KK=KK+1
   30 WRITE(3,300)((VEL(I,J),J=1,11),I=1,KK)
      WRITE(3,400) PRESS(1),L,V,RAD
  100 FORMAT(5X,4HSUM5,11X,4HTIME,11X,5HTHETA,10X,5HPRESS,10X,4HPAVE,
     111X,4HPEND,13X,3HQ,13X,3HVIS)
  200 FORMAT (8E15.5)
  300 FORMAT (11E12.5)
  400 FORMAT (4E15.5)
      CALL EXIT
      END
```

APPENDIX B. PHOTOGRAPHS AND OSCILLOSCOPE TRACES

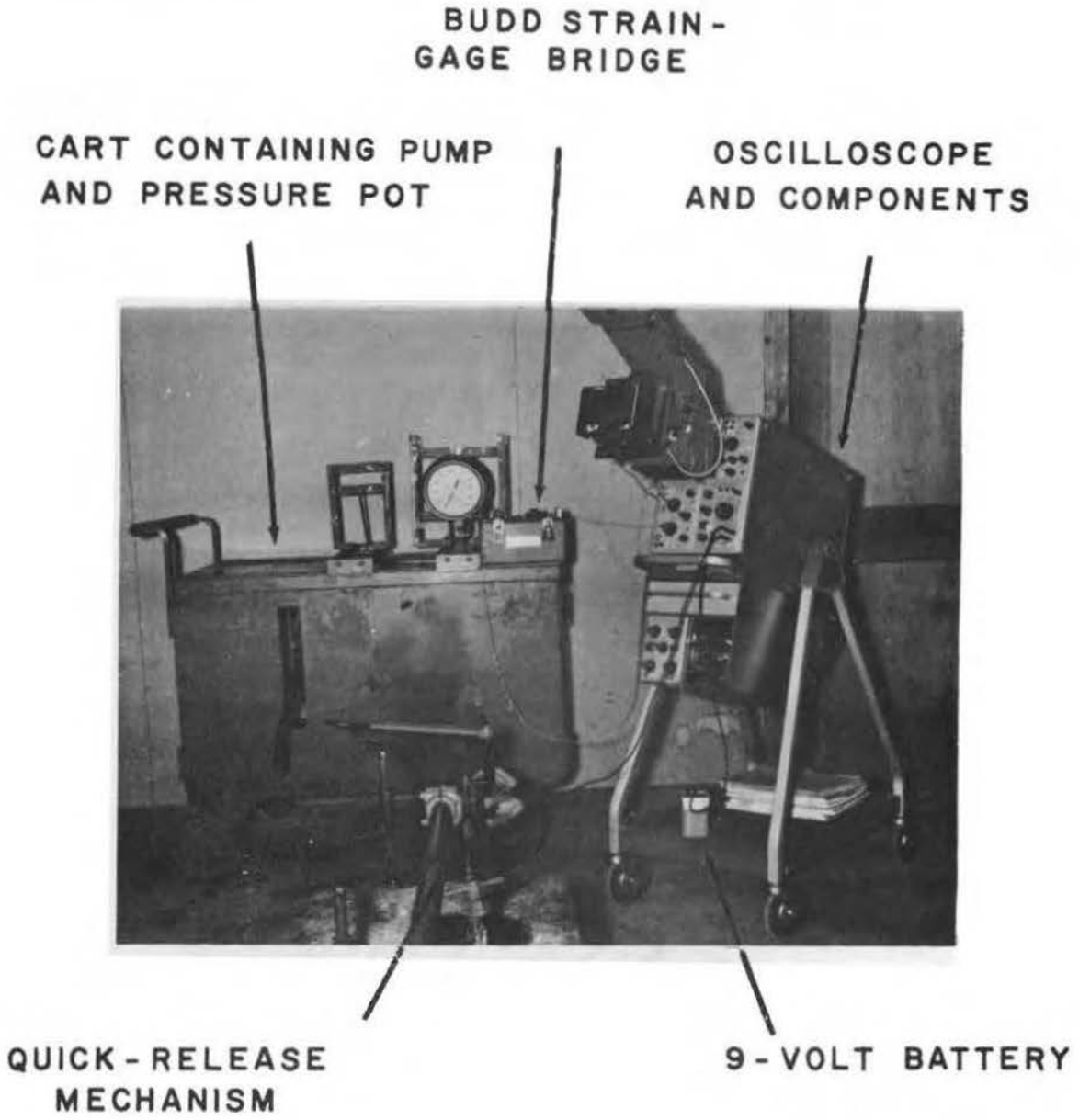

FIG. B-1 EXPERIMENTAL FACILITIES

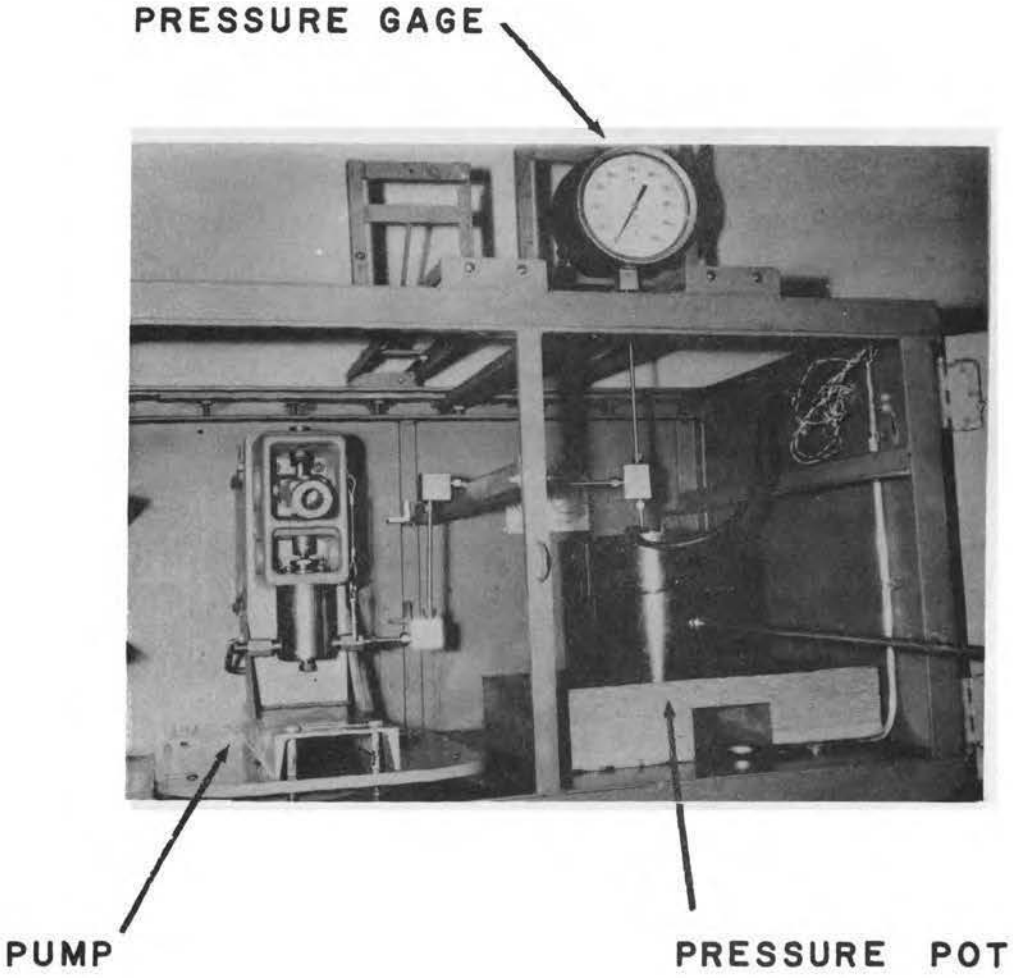

FIG. B-2 PRESSURE POT AND PUMP

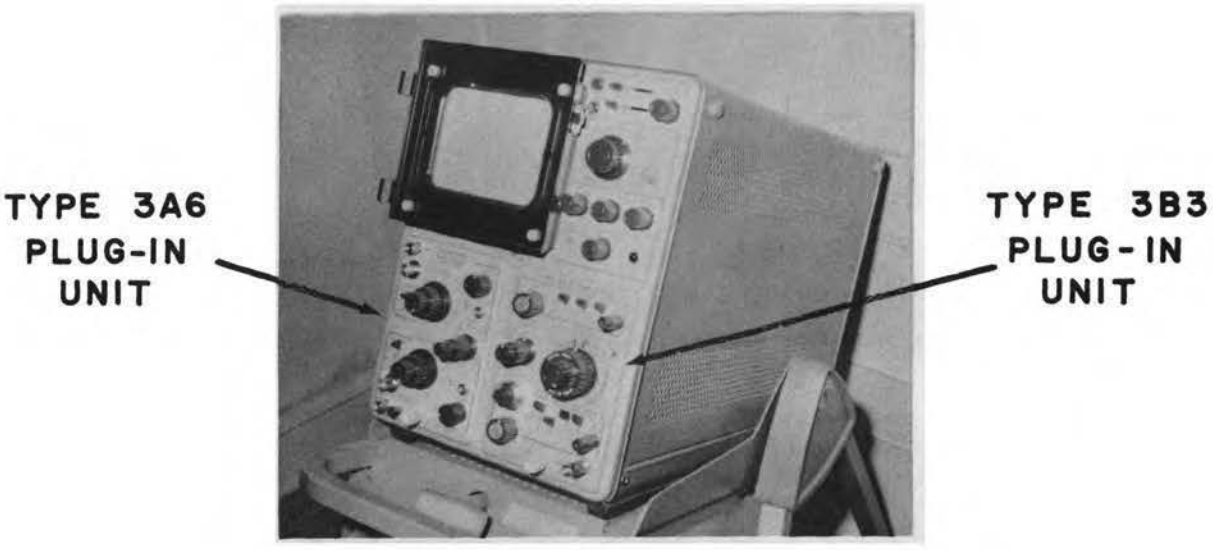

FIG. B-3 OSCILLOSCOPE AND PLUG-IN UNITS

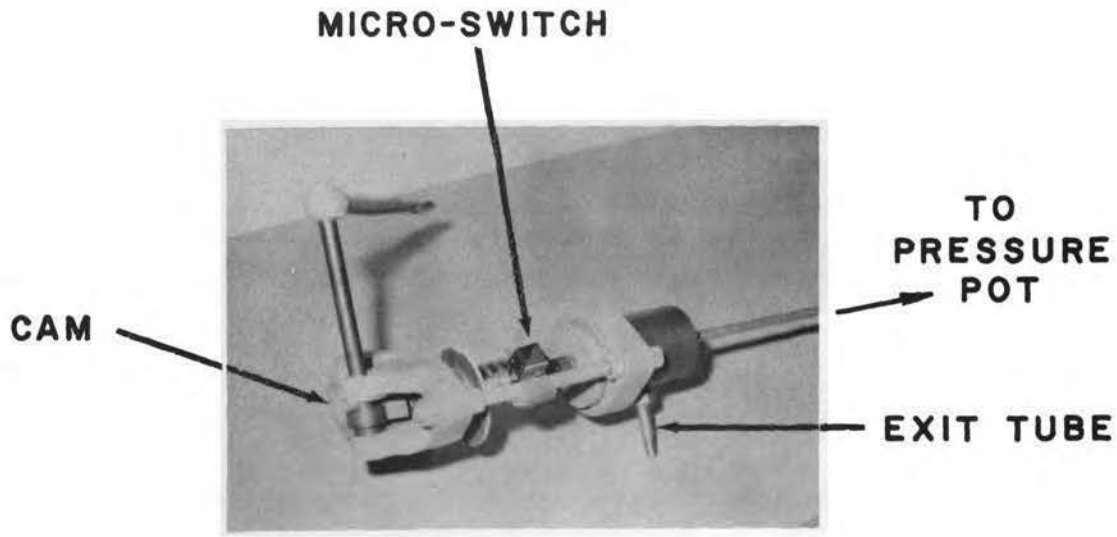

FIG. B-4 TRIGGERING DEVICE

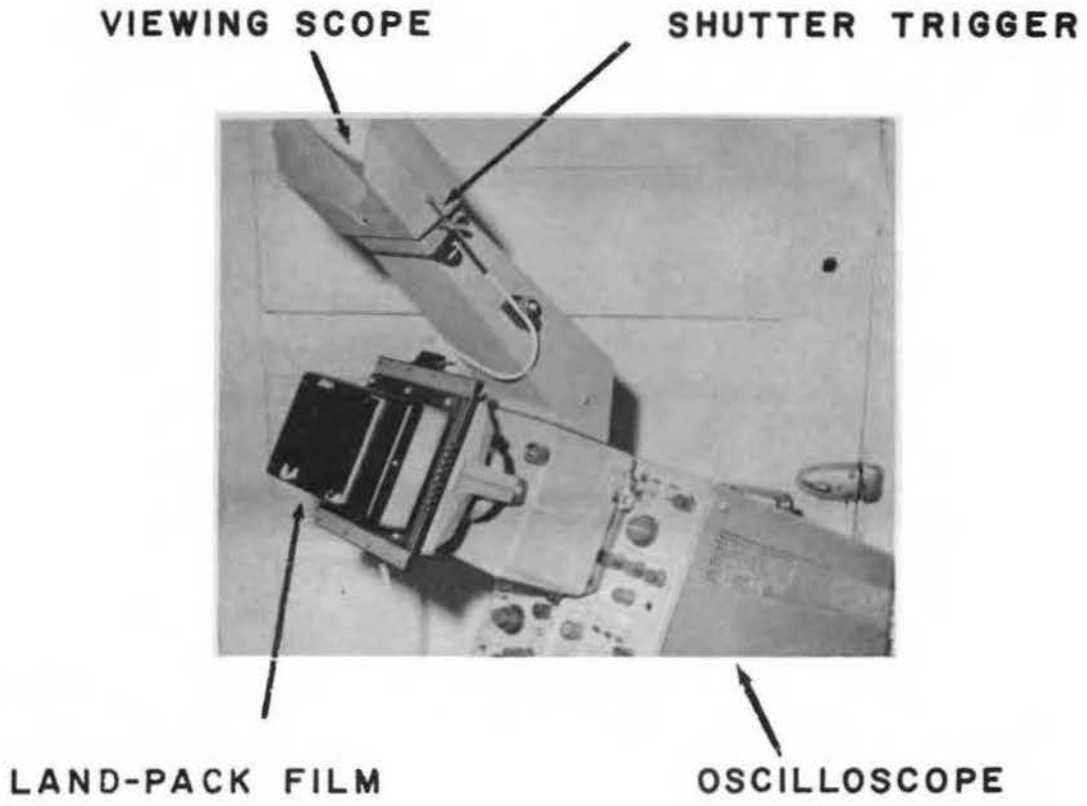

FIG. B-5 OSCILLOSCOPE CAMERA SYSTEM

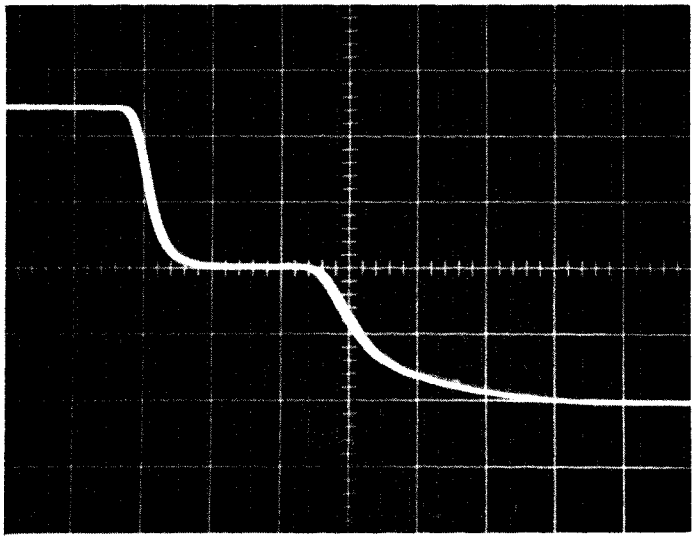

FIG. B-6 OSCILLOSCOPE TRACE (RUN NO. 6A)
INITIAL PRESSURE = 40,000 PSI
TIME / DIVISION = 20 MSEC.

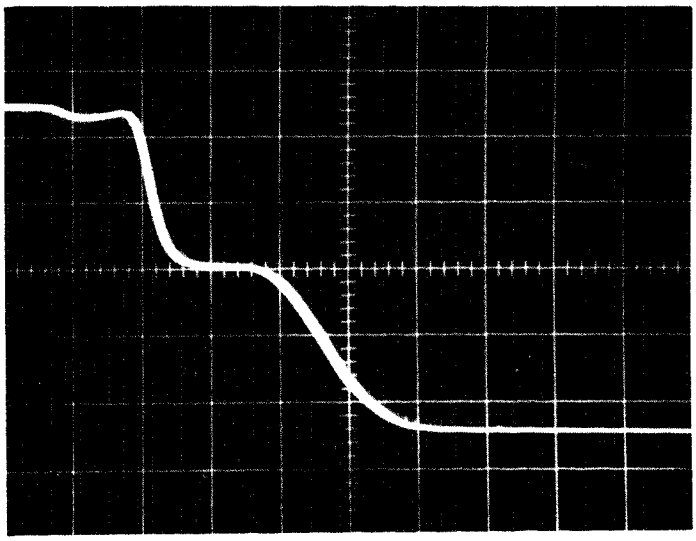

FIG. B-7 OSCILLOSCOPE TRACE (RUN NO. 8B)
INITIAL PRESSURE = 50,000 PSI
TIME / DIVISION = 20 MSEC.

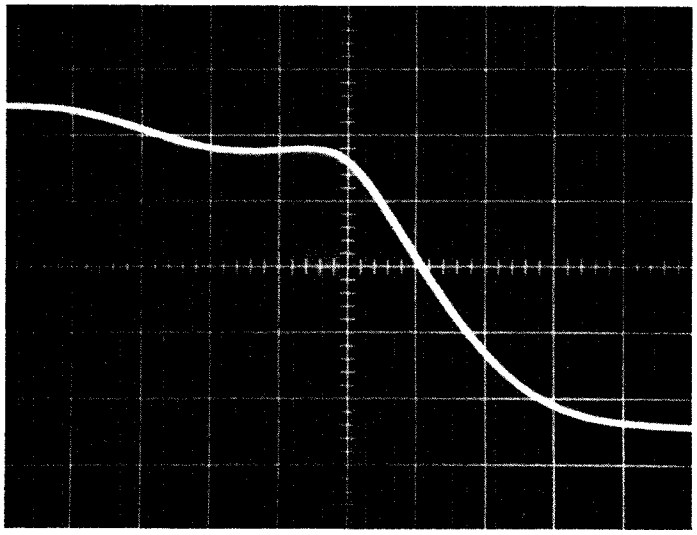

FIG. B-8 OSCILLOSCOPE TRACE (RUN NO. 24)
INITIAL PRESSURE = 50,000 PSI
TIME / DIVISION = 10 MSEC.

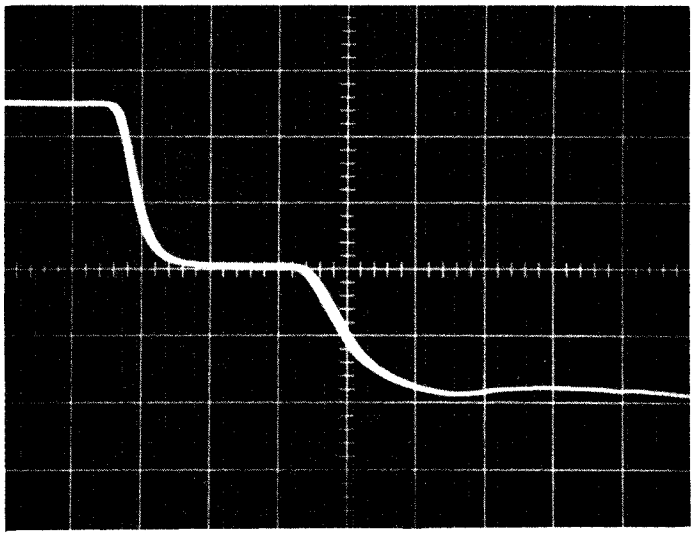

FIG. B-9 OSCILLOSCOPE TRACE (RUN NO. 27)
INITIAL PRESSURE = 40,000 PSI
TIME / DIVISION = 20 MSEC.

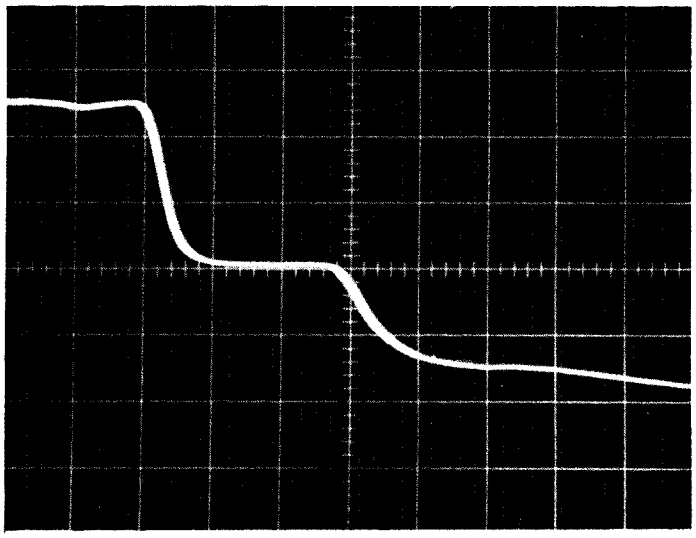

FIG. B-10 OSCILLOSCOPE TRACE (RUN NO. 28)
INITIAL PRESSURE = 45,000 PSI
TIME / DIVISION = 20 MSEC.

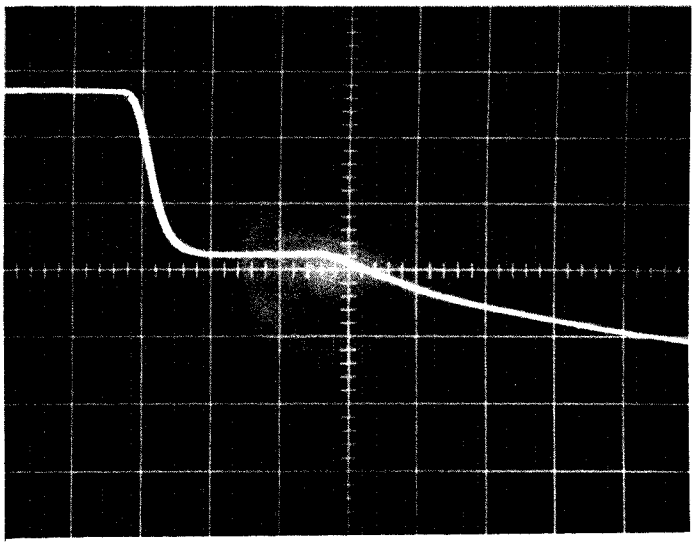

FIG. B-11 OSCILLOSCOPE TRACE (RUN NO. 31)
INITIAL PRESSURE = 20,000 PSI
TIME / DIVISION = 20 MSEC.

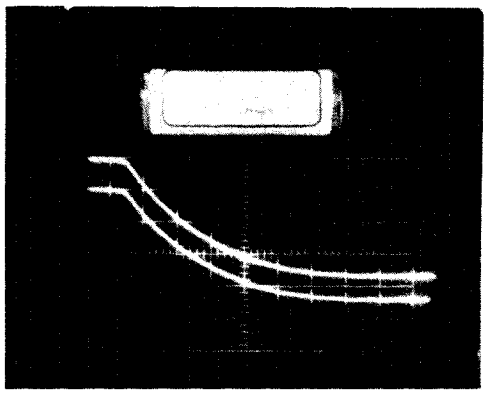

FIG. B-12 OSCILLOSCOPE TRACE (KNOCK-OFF TUBE)
INITIAL PRESSURE = 14,900 PSI
TIME / DIVISION = 5 MSEC.

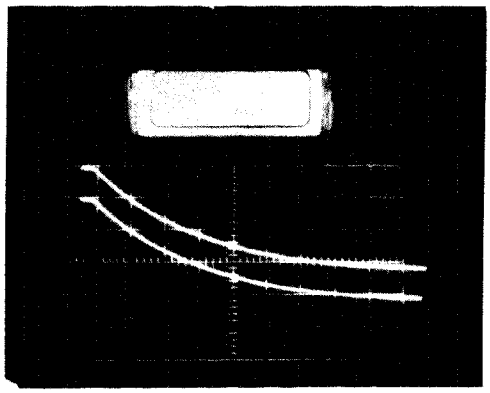

FIG. B-13 OSCILLOSCOPE TRACE (KNOCK-OFF TUBE)
INITIAL PRESSURE = 46,800 PSI
TIME / DIVISION = 5 MSEC.

APPENDIX C. DATA TRACES

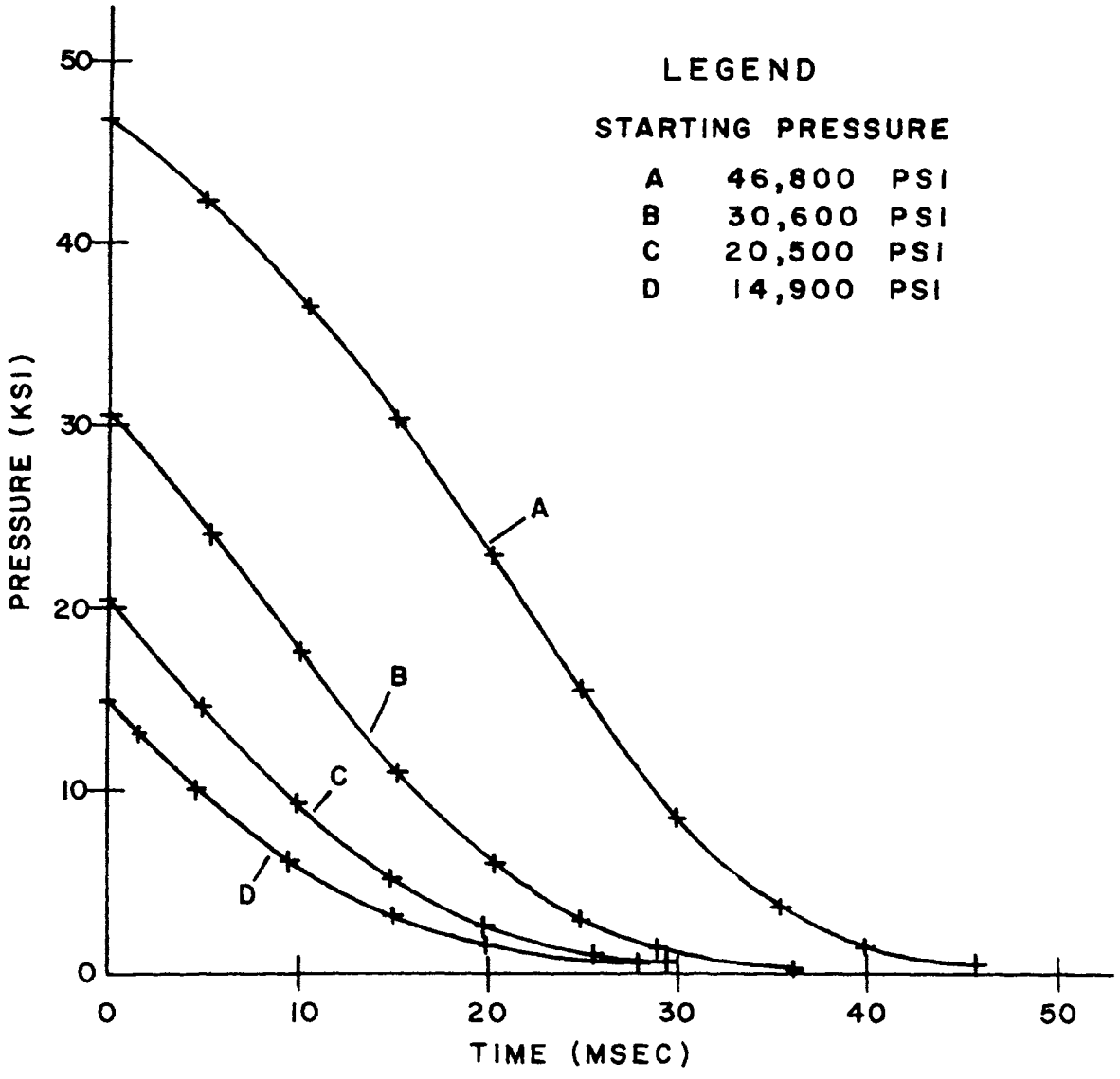

FIG. C-1 PRESSURE-TIME TRACES

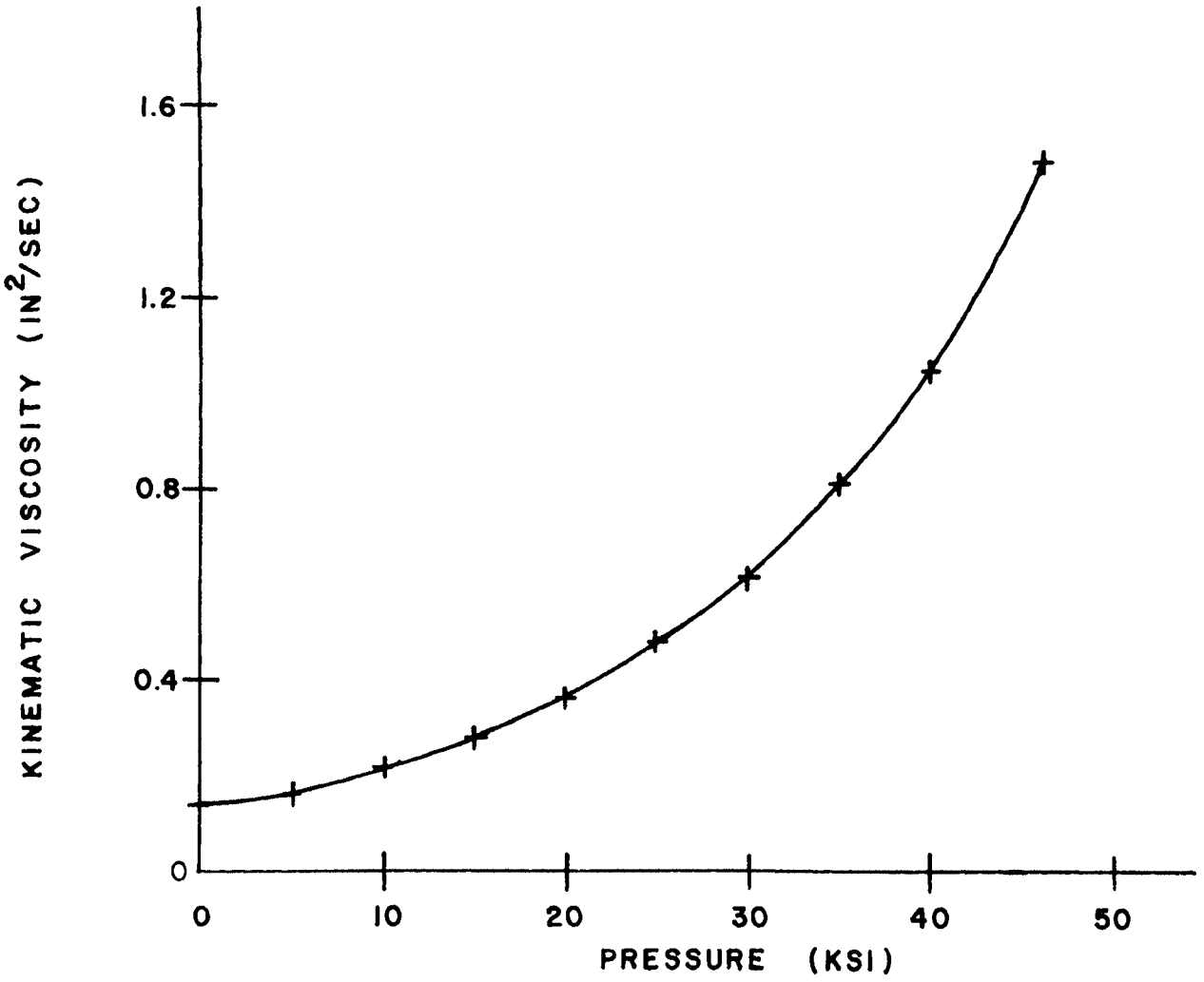

FIG. C-2 KINEMATIC VISCOSITY vs. PRESSURE

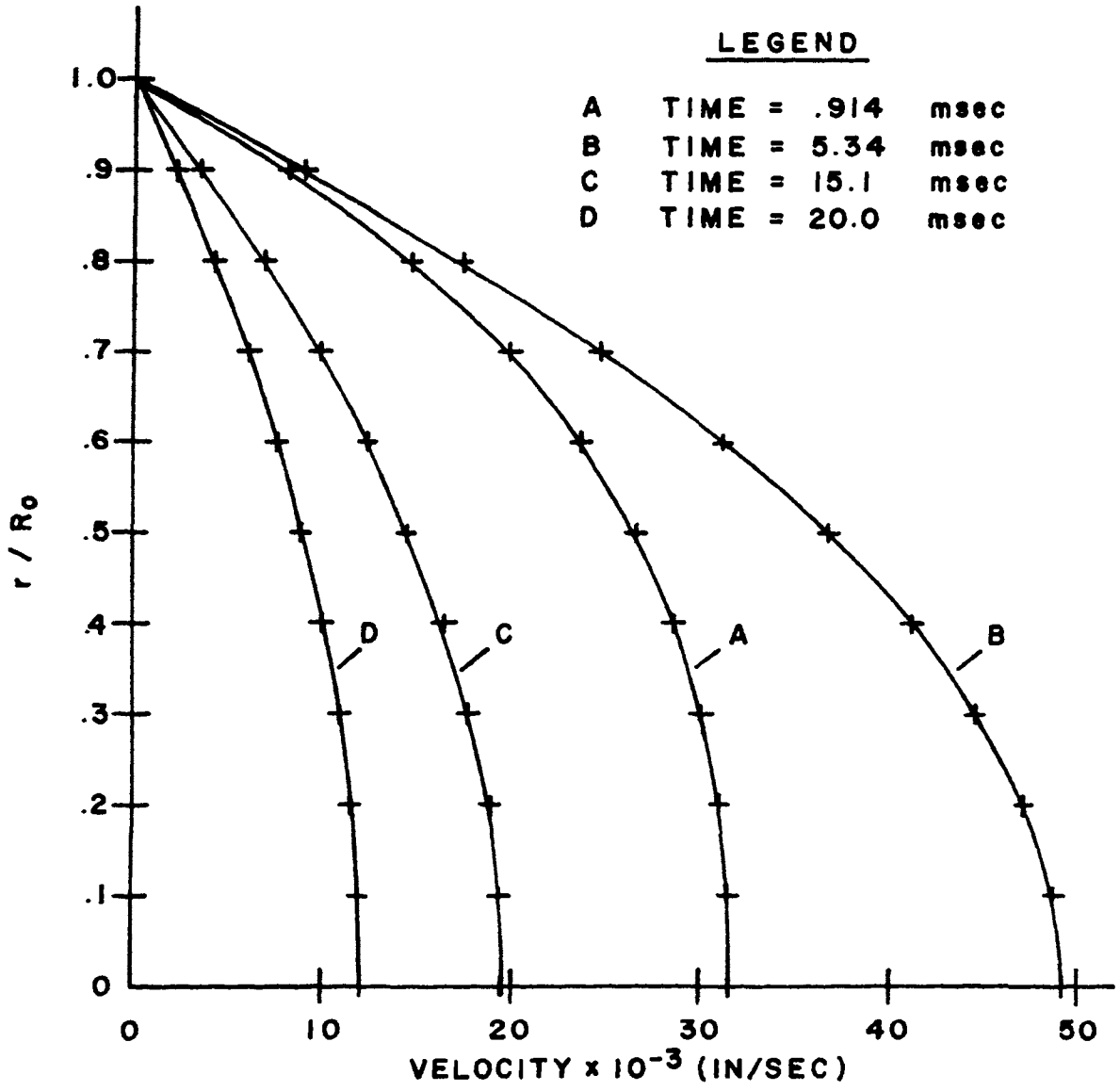

FIG. C-3 VELOCITY PROFILES FOR CONSTANT VISCOSITY (INITIAL PRESSURE OF 14,900 PSI)

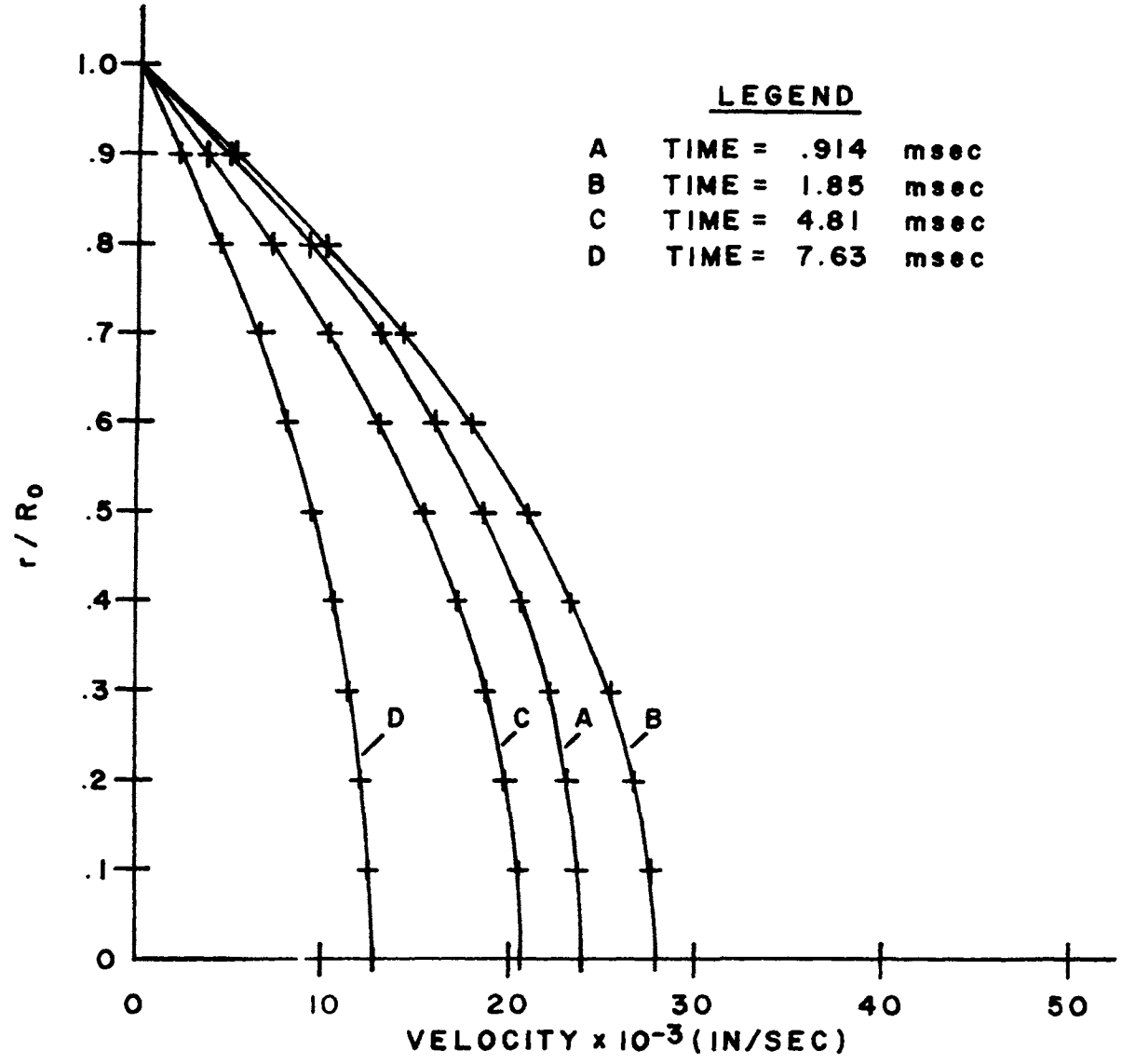

FIG. C-4 VELOCITY PROFILES FOR VARIABLE VISCOSITY (INITIAL PRESSURE OF 14,900 PSI)

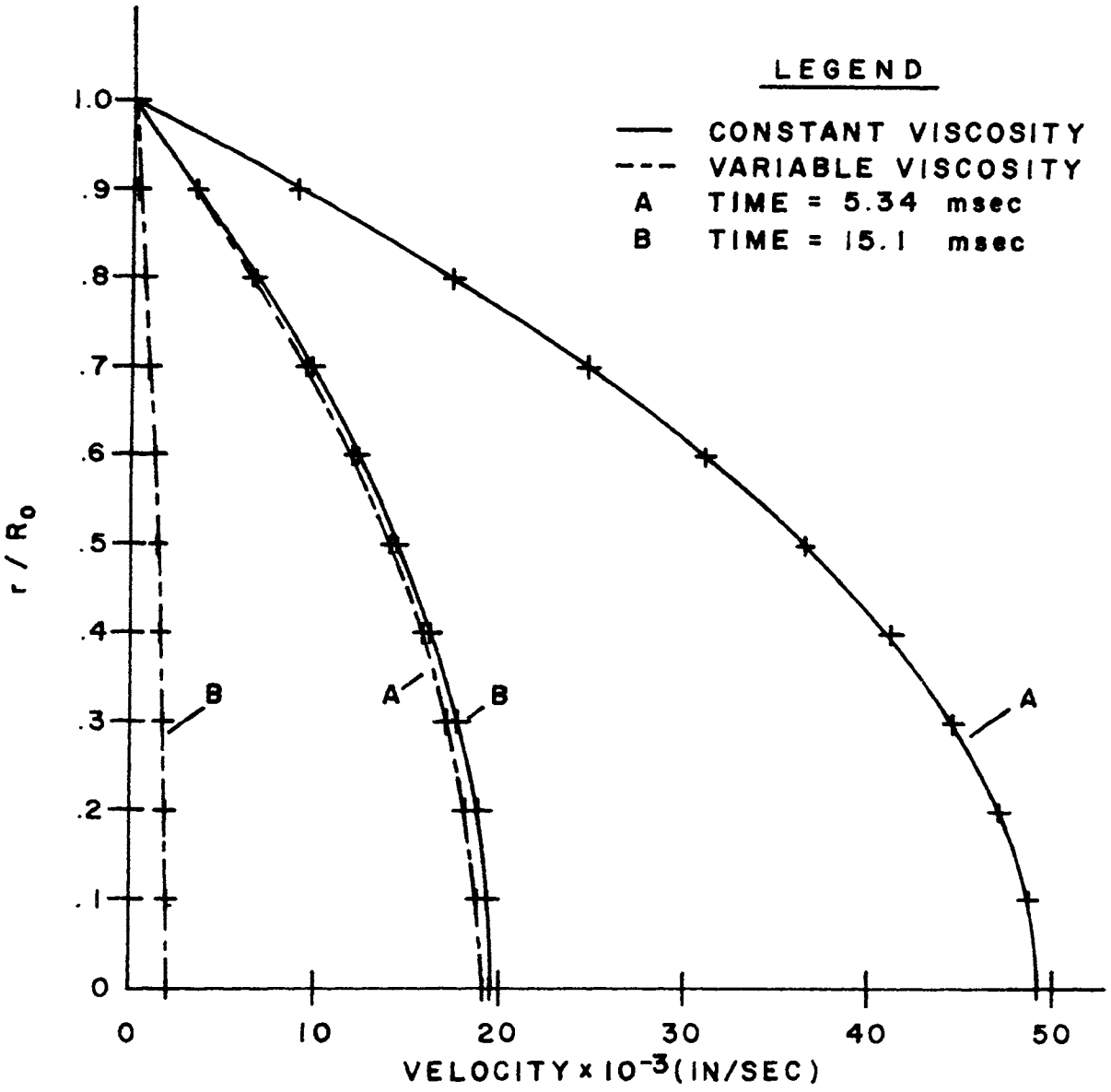

FIG. C-5 COMPARISON OF VELOCITY PROFILES (INITIAL PRESSURE OF 14,900 PSI)

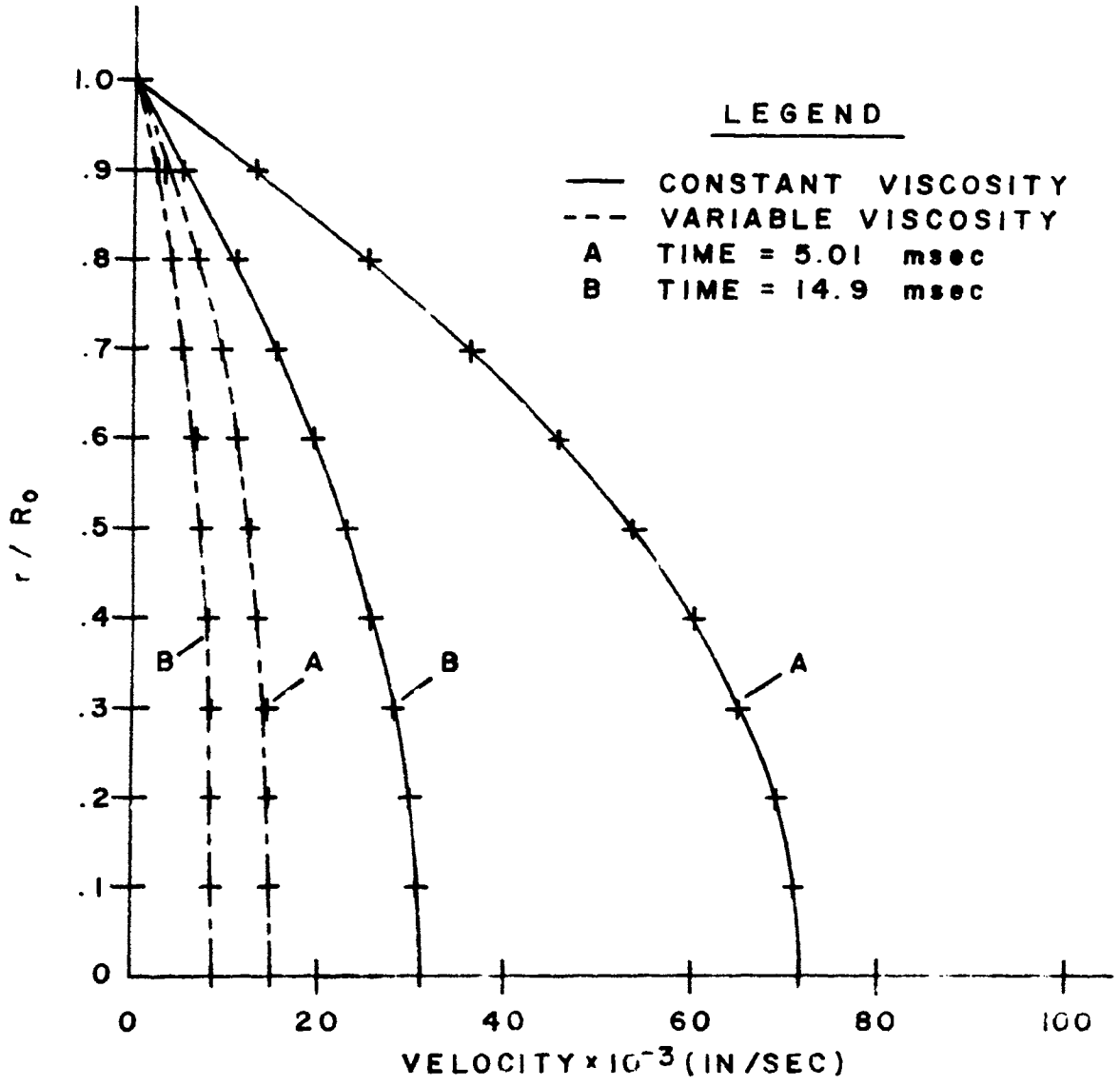

FIG. C-6 COMPARISON OF VELOCITY PROFILES (INITIAL PRESSURE OF 20,500 PSI)

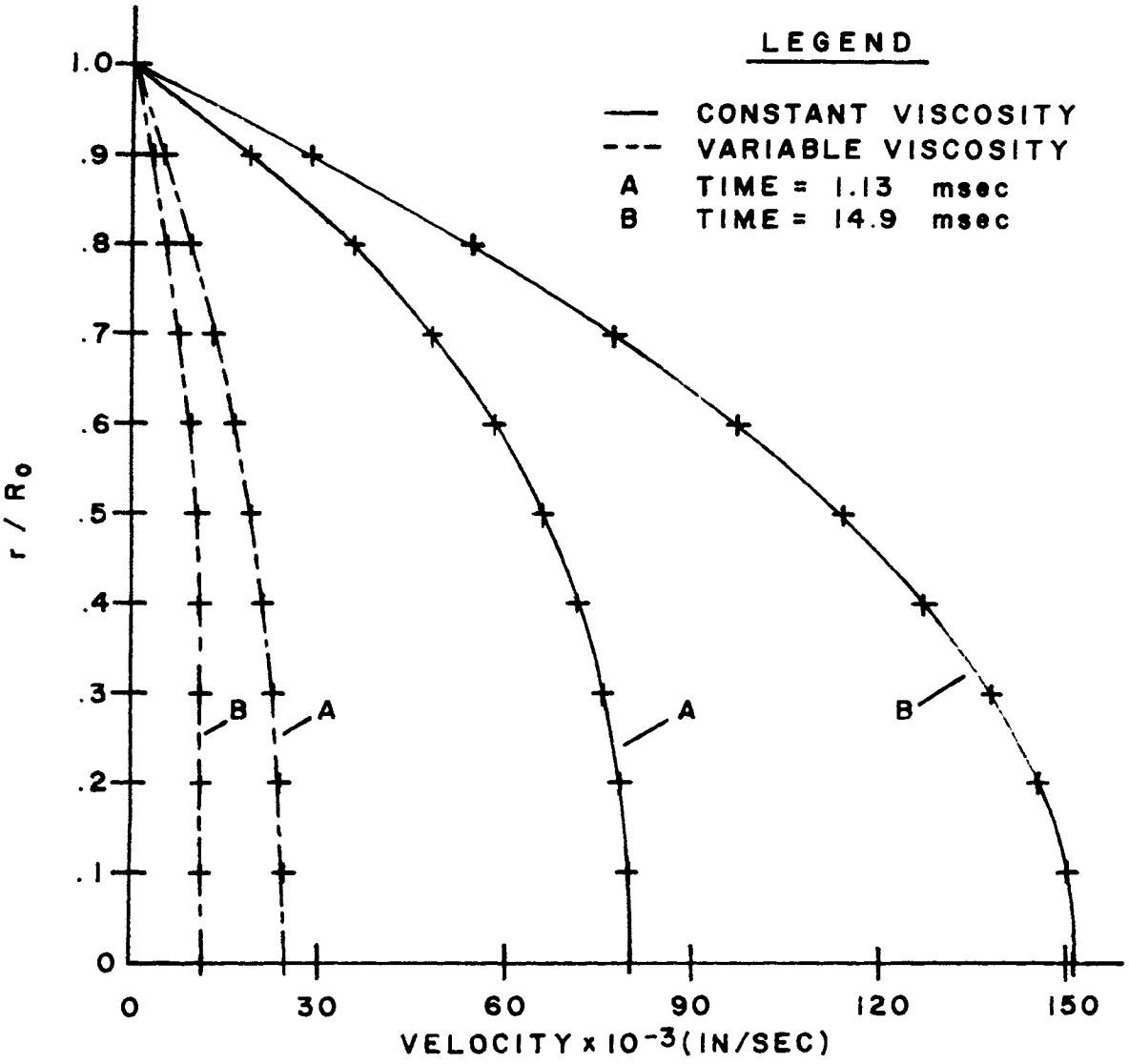

FIG. C-7 COMPARISON OF VELOCITY PROFILES (INITIAL PRESSURE OF 30,600 PSI)

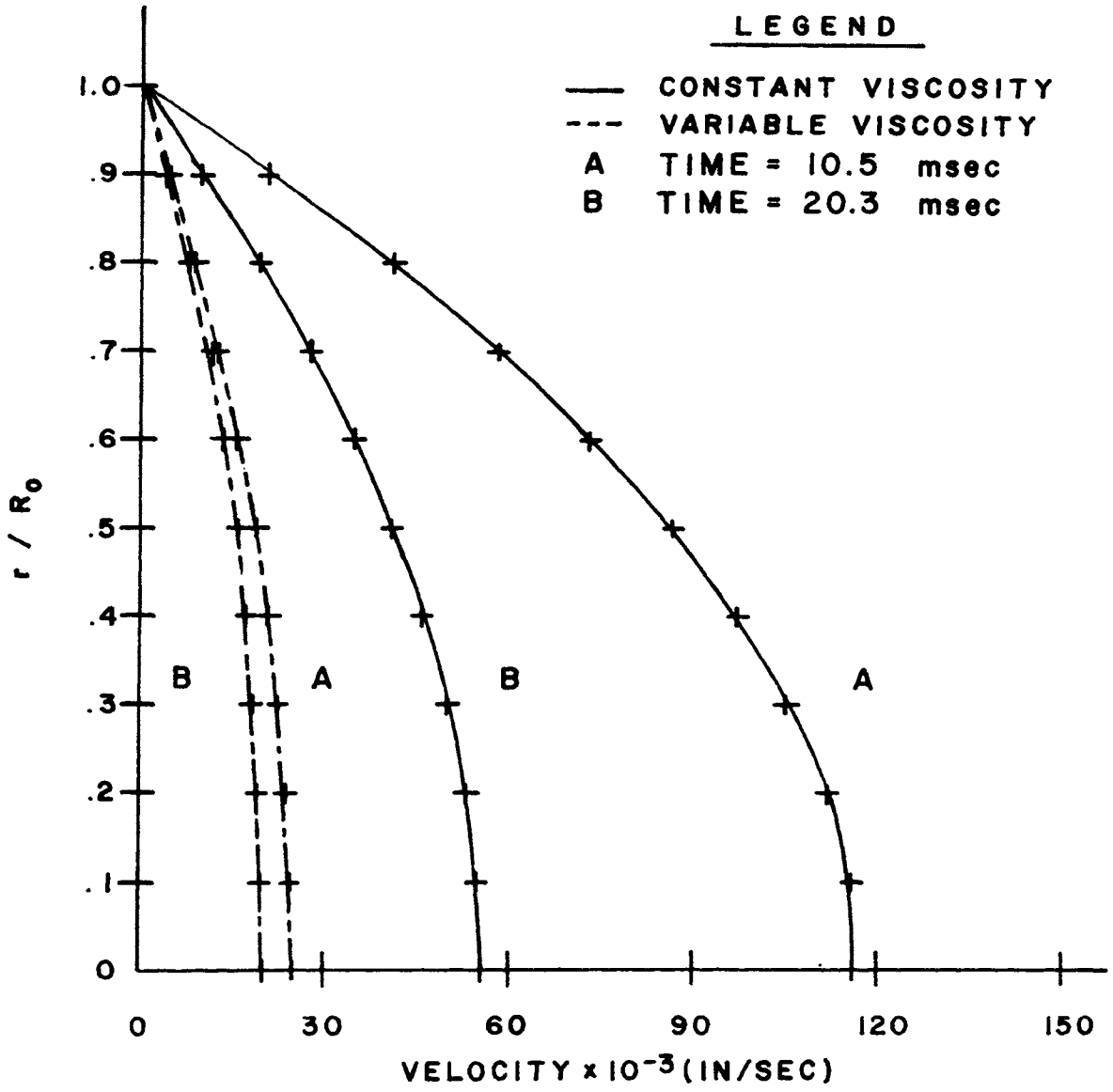

FIG. C-8 COMPARISON OF VELOCITY PROFILES (INITIAL PRESSURE OF 46,800 PSI)

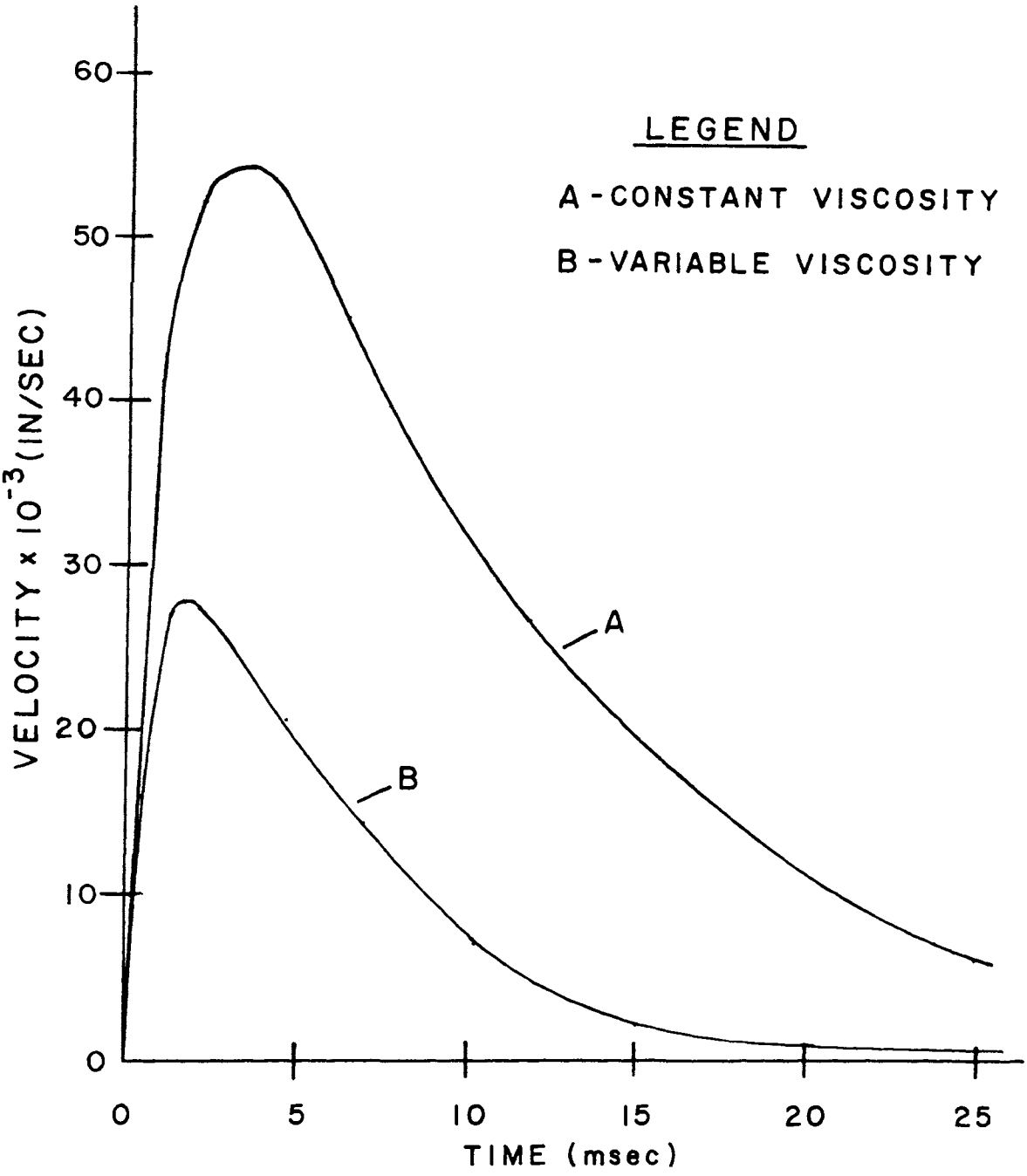

FIG. C-9 VELOCITY-TIME TRACES (INITIAL PRESSURE 14,900 PSI)

VI. BIBLIOGRAPHY

(a) Abramowitz, Mo. and Stegun, I.A., "Handbook of Mathematical Functions", Washington, D.C., National Bureau of Standards, 1967

(b) Avula, X.J.R., "Unsteady Flow in the Entrance Region of a Circular Tube", Ames, Iowa, Thesis to Iowa State University, 1968

(c) Davis, Robert L., "The Use of a Knock-Off Tube As a Quick Pressure-Release Mechanism", White Oak, Maryland, NOLTR 63-134, 1964

(d) Hersey, M.D. and Hopkins, R.F., "Viscosity of Lubricants Under Pressure", New York, The American Society of Mechanical Engineers, 1954

(e) Weiner, W.O., "Some Measurements of High Pressure Lubricant Rheology", Ann Arbor, Michigan, The American Society of Mechanical Engineers, 1968

(f) Miner, D.F. and Seastone, J.B., "Handbook of Engineering Materials", New York, 1955

(g) Condon, E.U. and Odishaw, Hugh, "Handbook of Physics", New York, 1958

VII. VITA

Robert Charles Weber was born on March 14, 1944 in St. Louis, Missouri. He received his primary and secondary education in Jennings, Missouri. He has received his college education from the University of Missouri at Rolla. He received his Bachelor of Science Degree in Applied Mathematics from the University of Missouri at Rolla in May, 1967.

He has been enrolled in the Graduate School of the University of Missouri-Rolla since September 1967.